École polytechnique fédérale de Lausanne

Semester Project

# Definition of design scenarios for the arrangement of tilted solar arrays and estimation of their electricity production from horizontal irradiances

*Authors :*
Adrien Legrain, MES
Sylvain Vitali, SIE

*Supervised by :*
Giuseppe Peronato
Sergi Aguacil
Prof. Marilyne Andersen

January 9, 2017

# Table of Contents

# 1 Introduction

Photo-voltaic solar production is growing very fast with the development of new technology and lowering of the cost of PV panels. In Switzerland, between 2010 and 2016, the solar production has been multiplied by more than 14 according to federal statistics [1] (see fig. 34 in Annexe). With this rising production, the interest of evaluate the overall potential of Switzerland has also known a great improvement. In 2002, the International Energy Agency estimated the maximal potential of photovoltaics to 25 GWp which correspond to a yearly production of 25 TWh [2]. To reach the maximal potential, 40% of the adequate roofs (=140 km$^2$) and facades (=55 km$^2$) would be covered by PV panel with an efficiency of 25 %. This estimation was quite rough and since 2002, the improvement in the solar potential assessment grows a lot ; in 2016 the Swiss national program *Toitsolaire.ch* appears in order to give for each building is solar potential (thermal or photovoltaics) [3]. To this assessment of the solar potential, several improvements still to be done and one is the estimation of flat-roof potential.

In *Toitsolaire.ch*, the solar potential of a flat-roof is defined by considering a horizontal irradiance on flat panels, which could lead to an overestimation of the solar potential. Indeed, it is possible to put more panels on a flat roof if they are horizontally aligned as there is no self-shading issue. However, in reality, panels are not generally horizontally settled on flat roof excepted Building-integrated photovoltaics (BIPV) (see fig. 1).

FIGURE 1 – BIPV on Stade de Suisse
Source : MyCityHighlight [4]

FIGURE 2 – Solar panels on EPFL roof
Source : Solstis [5]

When there are no aesthetic requirements and/or heritage protection on the flat roofs, the solar installations are generally tilted and oriented to the sun direction. On EPFL roof for example, solar panels are approximately spaced of 90 cm and tilted with a 18° angle (see fig. 2). Two main reasons explain this. First, panels are more efficient when tilted with an angle approaching the latitude [6], [7], [8]. Secondly, in practice the panels are tilted to avoid the deposit of dirt, leafs or snow, to favor the naturally cleaning of the panels by avoiding the deposit of dirt, leafs or snow and evacuate easily the water after rain [9].

The goal of this project is to elaborate a more realistic potential evaluation of solar production with the 3D-modeling of three different roofs including a high level of detail. Multiple evaluations according to different performance indicators are evaluated to reveal the optimal potential of three roofs situated in the urban environment of Neuchatel and compare it to the horizontal potential.

# 2 State of the art

One particularity of studying flat roofs solar potential is that the installation constraints are very weak compare to tilted roofs or façade installations where the aesthetic constraint is added to the geometric one [10]. As a result, the literature about installation codes on flat roofs is very broad and a quick review of already existing approaches is necessary. The table 1 resumes the main articles used in this project, specifies their scale of study and a short description of their utility in this project is done after the table.

| **Title** | **Author & Date** | **Scale** |
|---|---|---|
| Research of BIPV optimal tilted angle, use of latitude concept for south orientated plans [6] | Cheng et al., 2009 | Panel |
| Performance and feasibility assessment of a 1.4kW roof top grid-connected photovoltaic power system under desertic weather conditions [11] | Kazem et al, 2014 | Panel |
| The impact of array inclination and orientation on the performance of a grid-connected photovoltaic system [7] | Mondol et al., 2007 | PV array |
| A multi-objective assessment of the effect of solar PV array orientation and tilt on energy production and system economics [8] | Rhodes et al., 2014 | PV array |
| Optimal displacement of photovoltaic array's rows using a novel shading model [12] | Castellano et al., 2015 | PV array |
| A method to calculate array spacing and potential system size of photovoltaic arrays in the urban environment using vector analysis [13] | Copper et al., 2009 | PV array |
| Empirical approach to BIPV evaluation of solar irradiation for building applications [14] | Cheng et al., 2005 | PV array |
| BIM-based PV system optimization and deployment [15] | Ning et al., 2017 | Building |
| Photovoltaics on flat roofs : Energy considerations [16] | Bayod-Rújula et al, 2011 | Building |
| Assessment of rooftop photovoltaic potentials at the urban level using publicly available geodata and image recognition techniques [17] | Mainzer et al., 2017 | Urban |
| Urban Acceptability of Building Integrated Solar Systems : LESO-QSV Approach [10] | Probst et al. 2011 | Urban |
| Study to examine the potential for solar energy utilization based on the relationship between urban morphology and solar radiation gain on building rooftops and wall surfaces [18] | Takebayashi et al., 2015 | Urban |

Table 1 – Papers related to PV installation and their scale of study

First of all, Cheng et al. [6] explains the link between the best tilt angle for solar panels and the latitude, but this is only for individual panels and not for installations. At the scale of PV installations, some studies observed that the rule of thumb (panels facing south with a tilt angle of 30° for the US latitude) was the most efficient, with a low dependence on azimuth angle. However, they didn't provide any information about the distance separating the arrays [7],[8].

A more concrete scenario consists of no shading from the front array between 10 a.m. and 2 p.m. at the winter solstice [12], [13]. This method provides a direct link between tilt of panels and the distance between them. This scenario however is absolutely not unique, since some other research prefer considering no shading at solstice only between 11 a.m. and 1 p.m., or even strictly at 12 p.m. [16], [19]. In a paper of ISE Fraunhofer studying the potential of German cities [17], another rule is followed (30° tilted panels with L/D = 2) and the PACER even provides a table of installation rules with various tilt angles and the corresponding distance between array [20].

Such a diversity of available scenarios can be explained by Bayod-Rujula et al.[16], which reminds how many performance indicators can be optimized on one single installation, and how geometrical parameters can be tuned differently according to the objectives of the installer. In addition, Ning et al. [15] also states that when design codes exist, they are more adapted to industrial plants with low environmental constraints such as surrounding shading or the presence of obstacles that are more likely to be found on flat roofs in urban environments. In Osaka, a decrease of the solar potential up to 21% could be due to such shading effects at urban scale [18].

As a result, assessing the solar potential of flat roofs first requires a precise description of the studied urban environment and then an adaptation of the arrangement to that environment. This adaptation should be done by optimizing performance indicators that follow the stakeholder preferences. Once the potential has been assessed for one roof, it should be compared to other roofs of the same town to define an average of the influence of the environment over the potential. In any case, the solar potential of flat roofs overcomes widely the simple approach of considering flat panels covering the full roof, as will be studied in first steps. In a second time, we will compare the results of this simplified potential estimation to the advanced one.

# 3 Methodology

The main purpose of this study is to evaluate the solar potential of a flat roof installation in an urban environment thanks to a numerical model based on various geometrical parameters. Once the advanced potential is estimated, we compare it to the classical approach for horizontal surfaces, with the intention of finding an average ratio between the advanced potentials we compute and the classical one. As presented in the chart below, our methodology follows next steps.

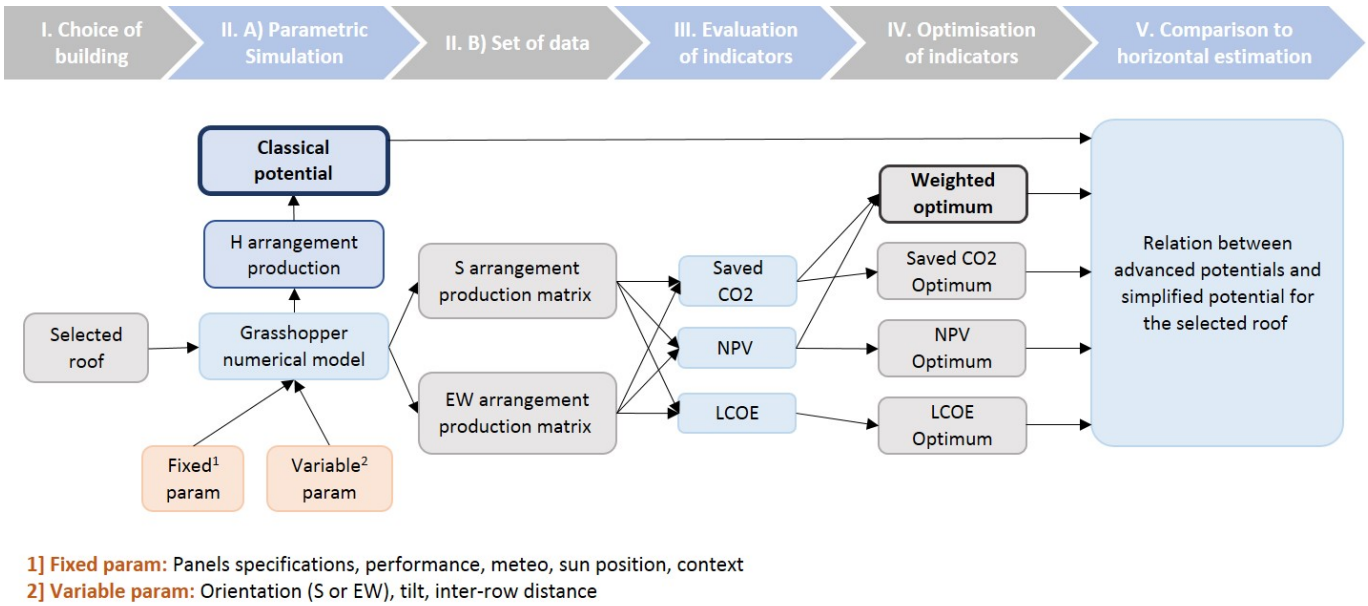


FIGURE 3 – Steps of the methodology

I We choose one building on which the simulation will be done.

II The geometry of the PV installation is automatically computed for different tilt angle and inter-row distances (IRD). For each set of parameter (tilt and IRD), the solar irradiation is used by the model to calculate the PV production. The results are stored into matrices, one for south orientation and one for east-west. This process is called parametric simulation in the present report.

III For each value of both production matrices, the indicators are computed.

IV For each indicator, an optimum is found through the 2 production matrices. Four advanced scenarios will be studied..

V A relation is established between horizontal scenarios and advanced ones. By comparing this ratio with the one of other roofs, a constant coefficient is obtained.

## 3.1 Studied buildings

During the project, 3 buildings have been studied. All buildings are situated in the urban environment of Neuchâtel. The latitude of the buildings is approximately 46°59' N and the longitude 6°56' E. The figure 4 shows the buildings in their surrounding environment. Two of the buildings are multi-storey apartments with shops at ground-level and one building is a garage. The names used in this project to differentiate the 3 buildings are :

— Garage
— Building
— House


FIGURE 4 – View from the south of the 3 buildings (Google Maps)

For each building, hourly electricity consumption is needed in order to compute the self-consumption, a necessary step in the calculation of the NPV indicator (see chapter 3.3.2). The norm SIA 2024 is used to evaluate the consumption profile of room and lightning electricity. Furthermore, it is assumed that all buildings are electrically heated with heat-pumps, domestic hot water included [1]. The hourly heating electricity consumption comes from heating simulation done with EnergyPlus from the paper of Aguacil et al. [21], [22]. Finally, a hourly electricity consumption per m$^2$ is obtained. To compute the total consumption per building, the following formula is used :

$$Hourly\ elec.\ consum. = Standard\ hourly\ elec.\ consum.\ per\ m^2 \cdot Roof\ area \cdot Storeys \cdot f \qquad (1)$$

Where $f = 0.85$, a factor to take into account the space not heated (staircase, ...).

### Garage

This building, called "Garage" in the project, is a garage parking space with a roof area of 459 m$^2$. The height of the garage is under the average and the horizontal irradiance is impacted a lot by the surrounding environment. The roof is flat with no chimney nor other obstacles. This garage has a nearly null electricity consumption and that is why, for the NPV indicator (see chapter 3.3.2), the electricity production of the garage is used in the apartment building situated in the south of the garage. The heated surface of this building is estimated to 1353 m$^2$.

1. This assumption support the hypothesis that solar installation could be installed during a complete renovation of old building


FIGURE 5 – View from the south of the garage (Google Maps)

### Building

This building, called "Building" in the project, contains 5 storeys of apartments and few shops at ground-level. Its roof top has an area of 591 $m^2$ and is at the same height or higher than the surrounding buildings. On the roof top, there is a stairwell and a lot of chimneys. The heated surface is estimated to 3014 $m^2$.


FIGURE 6 – View from the south of the apartment (Google Maps)

### House

This building, called "House" in the project, contains 4 storeys of apartments and a shop at ground-level. Its roof top has an area of 207 $m^2$ and is higher than the surrounding buildings. On the roof top, there is a stairwell and some small chimneys. The heated surface is estimated to 880 $m^2$.

FIGURE 7 – View from the north of the house (Google Maps)

## 3.2 3D Model and Parametric Simulation

The building environment seen on figure 4 has already been modeled in 3D by the Canton of Neuchâtel [23]. The 3D model of vegetation is also already present in the model and has been done with LIDAR according to Peronato et al. [24].

The complete model is opened on RHINOCEROS 5 (see fig. 8) and Grasshopper 3D is used to generate the geometry of the solar panels, applying a provided parametric model. Daysim (through the Honeybee plugin for Grasshopper) is used to simulate hourly irradiances on the PV panels.

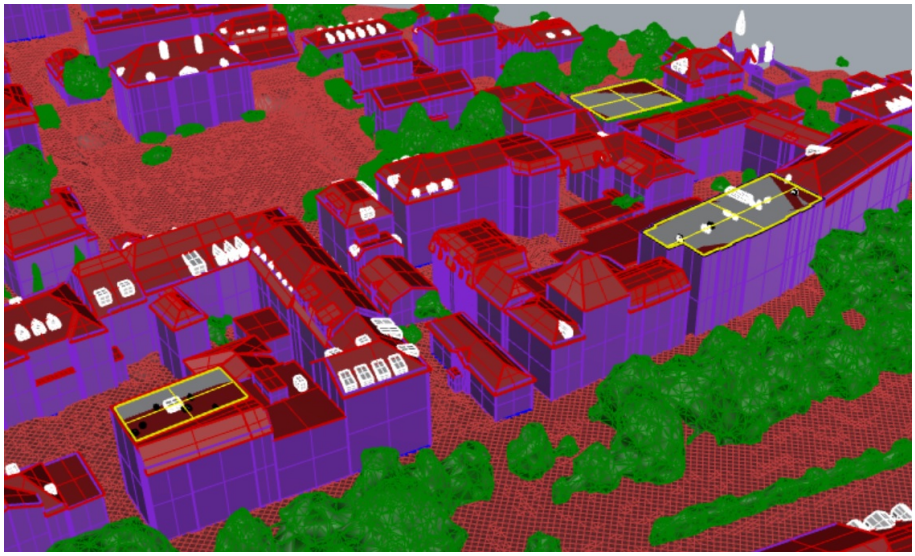

FIGURE 8 – Rhinoceros model - With the three roof (yellow surface)

### 3.2.1 Fixed parameters

Fixed parameters are the model inputs that are characteristic from the installation and its environment, but set unchanged during all the parametric simulation. In other words, these parameters are not tested in the optimization process, and so fixed at a value (or a set of values) found in an external source. They are composed of the context, panels specifications, installation performance, weather data and sun position.

#### Context

The context of an installation is the group of objects that are located in a close environment of the concerned roof. In the 3D model, the context of the roof can or not be taken into account. When

it comes to potential assessment, the context should be activated for more realistic results. In that case, a reflectivity coefficient is defined for each type of surface (see table 2).

| Element | Reflectivity [%] |
|---|---|
| Trees | 20 |
| PV panel | 10 |
| Roofs | 20 |
| Facade | 30 |
| Obstacles | 30 |

TABLE 2 – Surface reflectivity of the context

The context is not only important for the reflectivity of its components, but especially for the shading impact that some surrounding buildings or some obstacles can have on the installation. Moreover, the number of panels that can technically be installed on a roof with many obstructions is smaller than for a blank roof, decreasing the potential size of a PV installation for an obstructed roof. The level of detail of our final model was high enough to take into account all the chimneys and stairwells for the three roofs. Each panel was equipped with 16 irradiation sensors. If it didn't collect more light than a fixed threshold, then it was considered as covered by an obstacle and was deleted from the simulation. This parameter is considered as fixed since we will not test its contribution to the optimum (in real life, the panels don't have the choice between chimneys or not...). However, we could simulate different LODs of obstacles for the horizontal approach as explained below.

The garage is the only building impacted by trees. The trees situated above it (see fig. 5) are sources of shading on the roof, especially during the spring and summer when leafs are present. In autumn, the leafs fall and the effect of the trees become less important. To simulate this phenomenon from a mesh in RHINO, we assume that from the $1^{st}$ to the $30^{th}$ of October, the trees were present in the RHINO and that they were not present the rest of the year. As the total solar irradiance is 4.41 more important during the $1^{st}$ to the $30^{th}$ of October than for the rest of the year, the impact of the trees on the garage is quite important (fig. 35 in Annexe illustrates this effect).

### Panels specifications

The characteristics of panels have been defined in order to calculate the production of the solar installation.

The dimensions [2] of the panel is 1046 mm by 1558 mm which correspond to an area of 1.63 $m^2$. For the estimation of the solar production, an efficiency of 19.7% is assumed for the panels. To determine this efficiency, we first considered 21% efficient solar panels, and then applied a 1-diode PV production model including effective irradiance and temperature effect to simulate internal production losses of the panels [25]. As a result, we found that whatever the arrangement of the panels, the global generation of the installation tested was decreased by 6.19% for thermal reasons. Consequently, considering 21% efficient panels in real thermal conditions or ideal 19.7% efficient panels is the same.

The lifetime of the panel is estimated to 25 years, with a decay of the production along the panel life. The annual degradation rate of the production is 0.55 %, which correspond to 87% of the initial efficiency after 25 years [3].

In the advanced scenario, there are possibilities of shading between the arrays. To study this phenomenon and take it into account in the production estimation, we supposed that the panels are equipped of three bypass diodes (general case for mono-crystalline solar panels) so that the upper parts of one panel could produce while the lower is shaded and by-passed by the diode.

### Installation performance coefficient

2. The characteristics are inspired from the SunPower X21-345, one of the best panel on the market.
3. From the SunPower X21-34 warranty

In every PV installation, a performance factor is used to evaluate the global production taking into consideration external loss sources. These losses are mainly due to soil deposition on the panels with time, wires and contact losses in the electric system as well as the inverter performance which is estimated at 97% by ISE Fraunhofer. Moreover, leaves deposition due to the proximity of vegetation in the urban environment as well as snow in winter are other external sources of decrease in the performance of the installation.

When doing a brief review of the performance ratio in the literature, we conclude that 85% seems reasonable. Finally, we superpose the performance ratio to thermal losses estimated with Sandia model and to the predicted annual decrease of panels performance.

**Weather data and Sun position**

The weather data for irradiation simulation are coming from a historical review of Neuchâtel weather conditions published by METEONORM. They have been statistically sampled of a set of meteorological observations over the last 20 years. The sun position is also provided by METEONORM.

### 3.2.2 Horizontal approach for potential estimation

In some research and sun tools, the solar potential of flat roofs is estimated by considering the fixed parameters cited above and the surface of the roof as if panels were horizontally installed with a global performance coefficient [26], [16]. However, the rapid deployment of solar technology has forced counties to improve continuously the precision of their estimation models at urban scale [17], [18]. In order to address as many levels of detail as possible, it has been decided in this study to consider various horizontal scenarios as listed below from the simpler to the more detailed :

1. Aligned scenario : Flat panels aligned to the building, covering the whole roof. No detailed obstacles consideration. Surrounding buildings and vegetation consideration for shading.
2. South oriented scenario : Flat panels oriented to the South. 50cm empty space at the edges. No detailed obstacles consideration. Surrounding buildings and vegetation consideration for shading.
3. South oriented scenario + medium obstacles : Flat panels oriented to the South. 50cm empty space at the edges. Medium obstacles consideration such as stairwells. Surrounding buildings and vegetation consideration for shading.
4. South oriented scenario + medium + small obstacles : Flat panels oriented to the south. 50cm empty space at the edges. Medium and small obstacles consideration such as stairwells and chimneys. Surrounding buildings and vegetation consideration for shading.

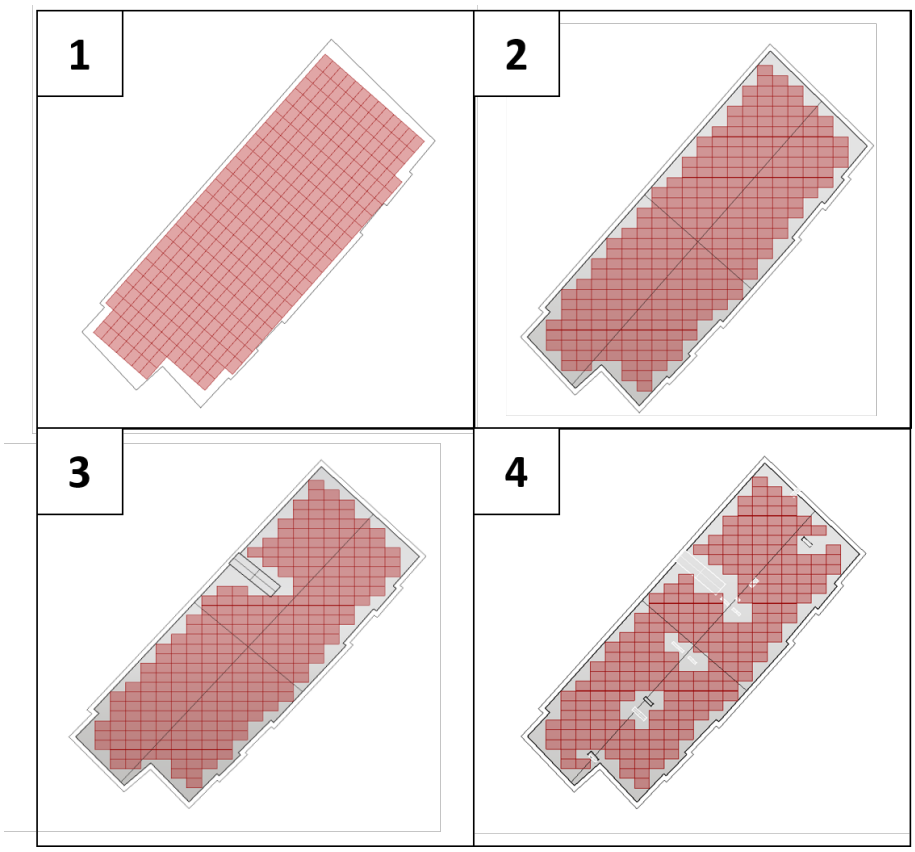


FIGURE 9 – Representation of the different horizontal scenarios on the Building roof

The advantage of the aligned and south-oriented scenarios are their easiness to be implemented with low level of information, which is adapted to quick estimations. Indeed, once the roof surface is known as well as the global performance linked to all fixed parameters except the obstacles, evaluating the potential of the roof is straight forward, it follows next equation :

$$E_{yr} = Irr_{yr} \cdot S \cdot \eta_{inst}$$

where $E_{yr}$ represents the energy generated in one year by the installation, $Irr_{yr}$ is the annual irradiation over the roof considering potential shading from other buildings, $S$ represents the roof surface and $\eta_{inst}$ represents the overall efficiency, considering panels and installation cumulated performance.

All the south-oriented scenarios were proposed to be more representative of a real tilted installation facing the south. This scenario is a bit more sophisticated than the aligned one and required the use of a numerical model for the panels arrangement. The first south-oriented scenario only takes into account the Swiss law of keeping 50 cm of space between the arrays and the roof edges. The second one adds the inclusion of stairwells to the model, that could be detected by photometric imaging of the city of Neuchâtel. Finally, we had to add chimneys manually in the model because they are too small for automated detection.

All these horizontal scenarios of potential evaluation are actually simplified ones since they don't consider the necessity of tilting panels for decreasing infiltration risks and soil deposition. When tilted, solar panels have better irradiation from the sun, but each array needs to be spaced from the one in front because of shading effects resulting in less panels that receive more light. Finally, the real potential happens to be more complicated to evaluate, since the irradiation over the panels depends on their tilt angle which has an influence itself on the shading distance.

As explained in part 2, some tilted arrangement codes already exist but these methods remain qualitative, and the optimal arrangement is highly depending on geographical location as well as personal interest of the stakeholder. That is why our model of potential estimation uses parametric

simulation [4], evaluates precise performance indicators and maximizes them according to the preferences of a specific profile of stakeholder arbitrarily defined in chapter 3.3.

### 3.2.3 Variable parameters

In order to find the optimal arrangement, the first step is to define what are the variable parameters. These are the inputs of the model that can be tuned in order to find its best output. In our case, the flexible inputs are the tilt angle, the inter-row distance (IRD) as well as the azimuth orientation. The IRD is defined as the distance between the projection of a front panel and the bottom of the one behind. The tilt angle is defined as the angle between the horizontal plan and the inclination of a panel.

#### Azimuth orientation

Since it leads to a three-dimensional problem, we have chosen to limit the variations of the azimuth to two possible orientations only, knowing this parameter has a low influence on panels production. These two possibilities are whether orientating solar arrays to the south (fig. 10), or adjoining two rows per array, one facing the east and the other the west (fig. 11). This arrangement takes advantage of the morning and evening sun and reduces the problem due to shadow from other panels, resulting in less geometrical constraints of installation.

FIGURE 10 – South oriented solar arrays
Source : Authors

FIGURE 11 – East-West oriented solar arrays
Source : Q CELLS [27]

#### Tilt and IRD

Now the problem is simplified to two dimensions, we have our two main variable parameters : the tilt angle and the IRD. In order to find the maximum output, we have to define a relevant set of inputs, defined by their extrema and their resolution. After a discussion with a professional of PV installation [9], the minimum tilt angle has to be set to 5° to avoid soil and water infiltration. By experience of previous simulations, the range of tilt angle have been defined between 5° and 26°, with a resolution of 1°. For the inter-row distance, knowing that it is possible to walk on solar panels without deteriorating them, we assume that the IRD can be set to 0m. Then, we have decided to push the model until reaching an IRD distance of 1.95m, with a resolution of 0.15m. Once the parametric area is defined, we can start to do some maximization of indicators under constraint.

### 3.2.4 Advanced approach for potential estimation

#### Bypass diodes in the model

4. At the beginning of the project, a theoretical approach has been tried, but has been abandoned. The result can be seen on chapter 9.1) in Annexe

In this part, we are studying the panels under various tilt angles and inter-row distances, which might lead to shading effects between consecutive arrays especially for south orientation. The shading effect on the PV production is modeled using panels equipped with a by-pass system [28]. On each panel, we assume that three bypass diodes are present and each panel is consequently divided into three groups of cells. Four irradiation sensors are equally spaced on the panel from the bottom to the top. Each group of cells is consequently attributed to two sensors. We consider the current generated by the group proportional to the lower irradiation between the two sensors. This selection of irradiation is repeated three times (one selected irradiation per group). At the end, an algorithm selects whether the shaded group should be bypassed or not in order to maximize the production.

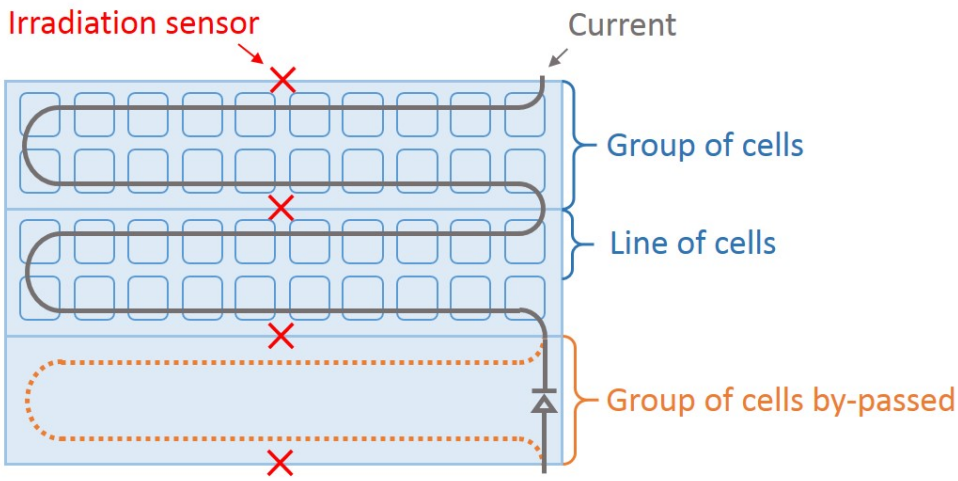


FIGURE 12 – Schema of the by-pass functioning in case of shadow at the panel bottom

### Parametric study

Now the model is reaching a high level of details, considering the use of by-pass diodes for facing shading issues and the variable parameters have been set, the electrical production is defined the same way as for the classical approach, but is calculated for each parametric step. For our given set of variables, it is possible to get a 3D surface illustrating an output indicator (e.g. the irradiation per installed $m^2$, the number of panels installed, the total production, ...).

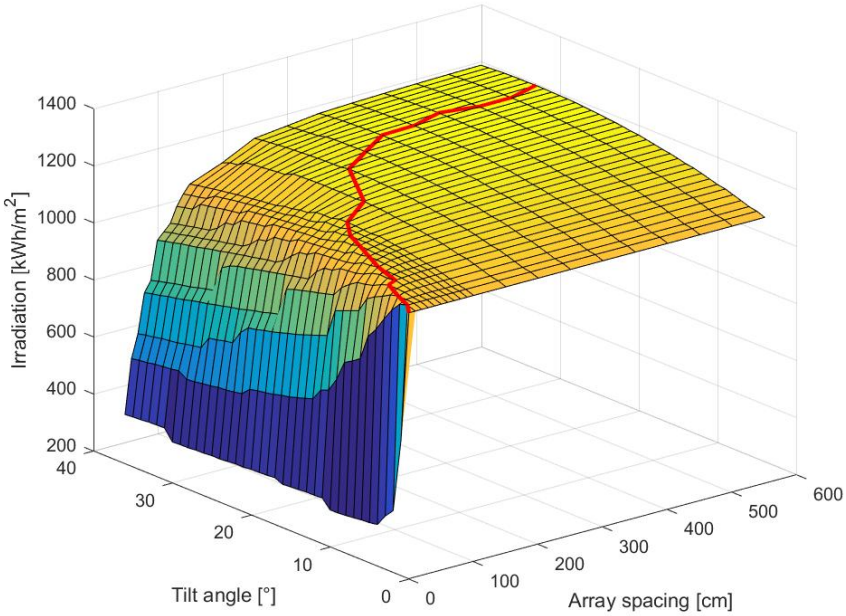


FIGURE 13 – Relation between tilt angle, IRD and irradiation

The red line can also be represented in 2D to show the best tilt angle for a given IRD (see fig. 14).

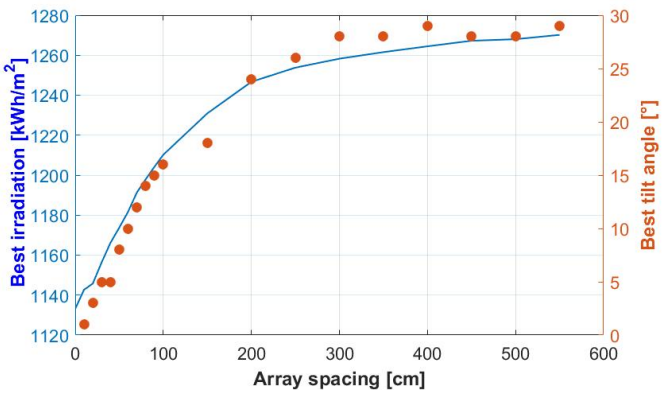


FIGURE 14 – Best irradiation and angle for a given distance

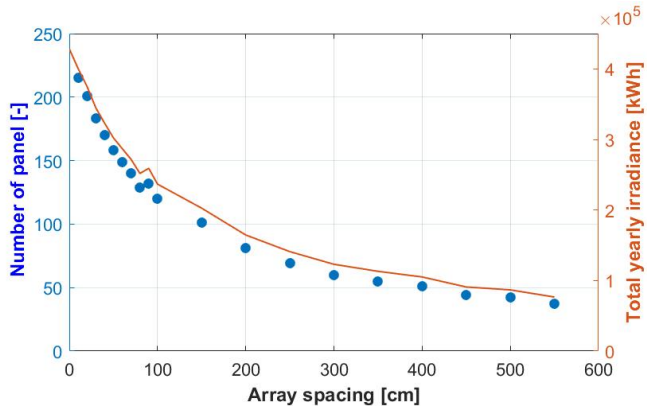


FIGURE 15 – Number of panel installed and total irradiation for a given distance

From this analyze, it is clear that the higher the array spacing, the higher the irradiance on the solar panel. However, a higher distance mean that less panels can be installed and that the total production will decrease (see fig. 15). The difficulty is to find the best compromise between a high efficiency of the panels and a high total production. To solve this question, different indicators have been explored in the next chapter.

## 3.3 Performance indicators

In the chapter 3.2.4, the relation between the angle and the array spacing has been computed, but it doesn't answer to which design is the best. To answer this question, four different indicators have been studied.

The two first indicators are economic indicators. The first one, Levelized Cost of Energy (LCOE) indicator is an economic assessment of the average total cost to build and operate a PV installation and aims to minimize the cost of production, that is the lower price per kWh of electricity produced.

This approach could be employed by an electricity retailer for example. The second indicator, the Net Present Value (NPV) calculates the value of a solar installation according to the benefit (electricity spared and electricity sold) and the cost of the installation. This approach could be employed by a private building holder who owns a flat roof and wants to lower its electricity expenses or even to make money with it.

The third indicator is an environmental indicator. The environmental optimization optimizes the installation in order to have the lower impact in term of $CO_2$ emissions.

The last indicator is a weighted indicator between the NPV and the environmental indicator. It gives a compromised result to the optimization.

### 3.3.1 LCOE Indicator

The Levelized Cost of Energy (LCOE) indicator is an economic assessment of the average total cost to build and operate a PV installation. This first approach aims to produce electricity with PV panels at the lowest cost possible. To do so, it uses 2 different aspects of PV installations. First, as shown in fig. 14, the more the panel installed, the more they are tightened and the less the efficiency per panel due to shading. Secondly, the more panels/power installed, the lower the cost per kWp installed due to economy of scale (see paragraph "Cost function" below).

By dividing the second relation by the first, it is possible to find a minimum. The figure 16 conceptualizes the research of an optimum.

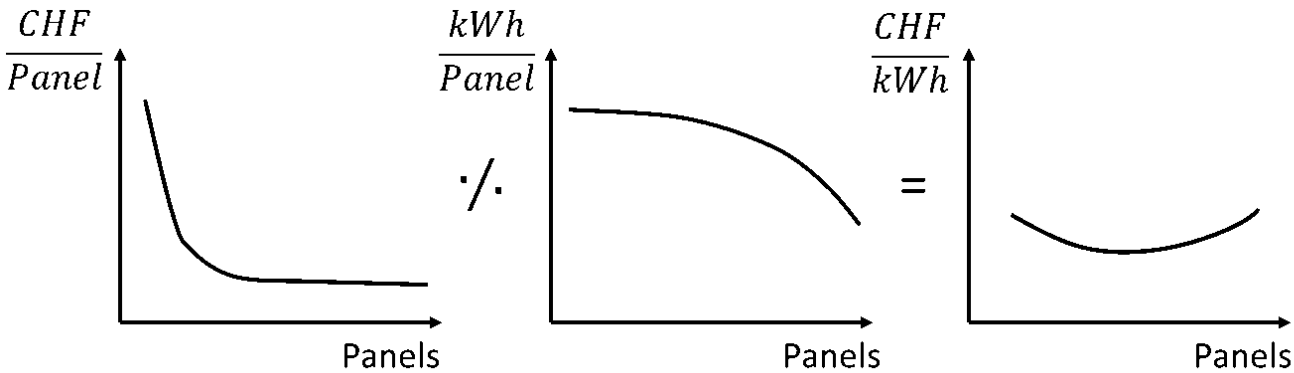


FIGURE 16 – Concept of the economical approach

#### Cost function

To evaluate the price of a PV installation, the SUISSEENERGIE calculator is used [26]. Simple in appearance, this calculator is well studied to evaluate rapidly the solar potential of an installation. The calculator also gives the expected total cost (turnkey solution) for installations between 2 to 150 kWp in Switzerland. Moreover, it is possible to see the expected federal subsidies and taxation deduction. From the result given by the calculator (see fig. 36 in Annexe), the total cost in function of installed power (or number of panel) has been deducted [5]. Two different costs are used according to the size of the installation :

If PV installation **lower** than 30 kWp : $$Cost\ [CHF] = 1800 \cdot kWp + 7200 \quad (2)$$

If PV installation **higher** than 30 kWp : $$Cost\ [CHF] = 1600 \cdot kWp + 13200 \quad (3)$$

For both sizes, the cost is given by a high initial cost and then a constant price per kWp installed. For a big installation (>30kWp), the price per panel is a bit lower (-11 %), but the initial cost of the

5. Although it has not been used, real market data of the MEGASLATE panel model can be compared in the fig. 37 in Annexes

installation is higher (+83 %). From those equations, it is clear that the more panels/power installed the less the cost per panels/power installed. The figure 17 shows the evolution of the price per kWp installed in function of the power installed. This function is used to look after a minimum cost of production as explained in figure 15.

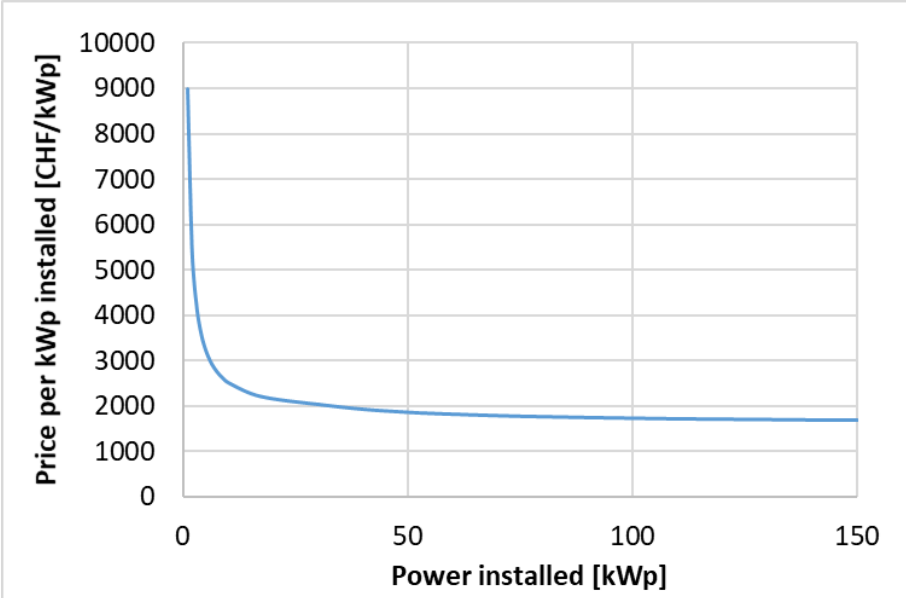


FIGURE 17 – SUISSEENERGIE DATA - Evolution of cost per power installed

Finally, the costs are annualized to obtain a constant price for the electricity produced during the lifetime of the panels. The following formula is used :

$$Annualized\ cost\ [\frac{CHF}{year}] = I \cdot \frac{i(1+i)^n}{(1+i)^n - 1} \tag{4}$$

The initial investment $I$ is given by the cost function, the expected lifetime $n$ of the panel is 25 years and the discount rate $i$ is 5% [17]. In our evaluation of the cost of electricity, we suppose that a certain quantity of electricity will be generated, however, there are risks that the panels get deteriorated faster or that the company supplying panels goes bankrupt and then the panels are no more ensured in case of damage for example. The discount rate is here to take these risks into account and re-evaluates the cost a bit higher.

### 3.3.2 NPV indicator

The Net Present Value (NPV) indicator represents the discounted value of the cash flows of the project. In order to calculate the NPV, we need to compute first the initial investment and then to discount all the future promised cash entries. In the cost function of the NPV indicator, in order to match more with the investment of a private installer, the possible subsidies and fiscal deductions are added in the equations 2, 3 of the price used in the LCEO indicator. Therefore, the cost in function of the power installed is lower than in the LCEO indicator. The subsidy used is the unique contribution [6] [29], even if another subsidy exists [7] for installation bigger than 100 kWp [30].

According to the SUISSEENERGIE calculator, unique retributions don't change if the installation power is higher or lower than 30 kWp and worth :

$$Subsidies\ [CHF] = 400 \cdot kWp + 1400 \tag{5}$$

6. In French : Rétribution unique (RU)
7. In French : Rétribution à l'injection, anciennement Rétribution à Prix Coûtant (RPC)

A second possible reduction of the initial cost (formula 2, 3) is the fiscal deduction during the year of installation. This deduction can reach 20% of the initial tax depending of the Canton. The SuisseEnergie calculator also gives an estimation of this deduction in function of the power installed and in function of the installer annual salary. From the result given for a mean Swiss salary of 80'000 CHF/year, the following tax deduction could be expected in function of the power installed :

$$Fisc.\ deduc.\ [CHF] = 2.2 \cdot 10^{-4} \cdot kWp^4 - 0.0264 \cdot kWp^3 - 1.785 \cdot kWp^2 + 306 \cdot kWp + 1997 \quad (6)$$

The curve of the fiscal deduction is shown in figure 18. After 50 kWp installed, the fiscal deduction stabilizes and even decreases a little to reach 10'000 CHF/kWp.

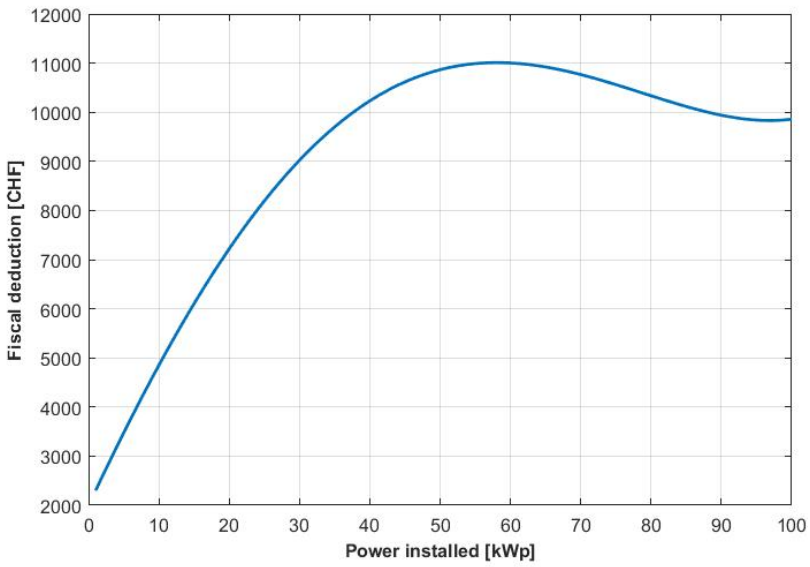


Figure 18 – Fiscal deduction in function of installed power peak for a mean salary

The final cost according to the power installed is obtained by subtracting 5 and 6 to 2 or 3, according to the size of the installation. Since both subsidies are theoretically paid in the first year, there is no need for discounting them. It is remarkable that both subsidies are encouraging investors to install more panels as they are growing functions with the size.

Once the subsidies are added to the initial investment, we can evaluate how much money is going to be saved or earned in the next years, and discount for the same reason as LCOE. In this scenario, we suppose that our three buildings self-consume the energy produced on their roof, and when too much electricity is generated, the surplus is sold to the grid. As a result, the two expected cash entries are going to be the money earned when sold to the grid (feed-in tariff) and the money saved by self-consuming the electricity produced by the installation, which is generally cheaper than the Swiss electricity price.

In Neuchatel, the feed-in tariff for installations smaller than 30 kWp is fixed at 11.8 $ct_{CHF}/kWh$ ($t_{small}$), and approximately 6.85 $ct_{CHF}/kWh$ for bigger installations ($t_{big}$). The money saved thanks to self-consumption is considered equal to the Swiss electricity price in Neuchatel canton : 21.69 $ct_{CHF}/kWh$ ($p_{swiss}$) [31]. The discount rate **i** is the same than in LCOE indicator and equal 5%. The discounted cash flows for year $n$ sum the money saved to the money earned as shown in next equation :

$$\text{If PV installation } \textbf{lower} \text{ than 30 kWp :} \quad DCF_n = \frac{E_{sc} \cdot p_{swiss} + E_{sold} \cdot t_{small}}{(1+i)^n} \quad (7)$$

$$\text{If PV installation } \textbf{higher} \text{ than 30 kWp :} \quad DCF_n = \frac{E_{sc} \cdot p_{swiss} + E_{sold} \cdot t_{big}}{(1+i)^n} \quad (8)$$

In previous equation, $E_{sc}$ is the self-consumed electricity and $E_{sold}$ is the electricity sold to grid.

The equations 7 and 8 above highlight a characteristic phenomenon of self-consumption. We can see in these equations that the ponderation of self-consumption in the present value of future cash flows is three times higher than the contribution of the electricity sold to the grid. As a result, self-consumption is much more contributing to future cash entries than the overproduction. However, since the production of a big PV installation is overcoming the quantity of electricity consumed during the day, the fewer the panels installed, the higher the part of self-consumption in the overall electricity generated. This phenomenon should create an incentive to produce less, that will be verified in the results.

### 3.3.3 $CO_2$ indicator

With this indicator, we suppose that the co-owners of the building are ecologists caring more for the environment and future generations than for their money. The more common parameters for studying environmental impact are the avoided $CO_2$ emissions and the energy payback time of the panels according to their productivity during their lifetime. We have chosen to study only $CO_2$ avoided because the energy payback time is less concrete to evaluate the environmental impact, it is a more abstract indicator than the number of carbon emissions in the atmosphere that are concretely avoided.

The carbon avoided is evaluated as follows : supposing my solar installation has produced a quantity Q of electricity, we compare the carbon that has effectively been emitted by the solar installation to the carbon that would have been emitted if it had been produced by the Swiss power mix or importations. Two factors have consequently been studied : the carbon intensity of our solar panels as well as the one from the substituted source of electricity.

For our installation carbon intensity, we have drawn on a research doing a full LCA of Sunpower panels at 20% efficiency. According to Fthenakis et al. [32], one Sunpower panel has a carbon footprint of 1380 kg/KW, which leads to 48 gCO2/kWh considering Neuchâtel irradiation of 1160 kWh/m$^2$/yr and a lifetime of 25 years. This value is coherent with multiple studies of PV LCA approximating the average carbon footprint of a panel between 40 gCO2/kWh and 100 gCO2/kWh generated.

Since solar energy is an intermittent source, it can only substitute a flexible source. One common approach is to consider it substitutes importations from the German mix to the swiss grid. The mix of Germany is globally oscillating between 300 and 500gCO2/kWh because of a high contribution of coal plants [33]. By supposing an improvement of the German mix intensity until 25 years and to simplify the model, we have assumed that each kWh of electricity substituted would have an average carbon footprint of 300kWh.

### 3.3.4 Normalized Weighted indicator

This indicator is a mixed of the NPV indicator and the $CO_2$ indicator. When two indicators are used to study one project, a conventional approach could be to normalize them and then combine both[34]. In other words, we set the maximum value of the studied indicators to 1 and their minimum value to zero. Then, we choose arbitrarily to sum both with a weight of 1/2 each. As a result, the arrangement that allows the value closest to 1 is considered as the optimal one. Then since we have done this maximization both for south and EW orientation, it only remains to select the arrangement that has the higher overall indicator between the two.

# 4 Results

In this section, the result of the different indicators is described and discussed. For the sake of synthesis, only the Garage results are presented. For each indicator, the variable parameters are those defined in chapter 3.2.3 and the context is always activated. The effect of context is discussed in chapter 5.3.

## 4.1 Results for individual indicators

### 4.1.1 Results for LCOE indicator

As a reminder, the LCOE indicator represents the cost per kWh of electricity produced. The results of the Garage for the two different orientations are illustrated in the figure 19.

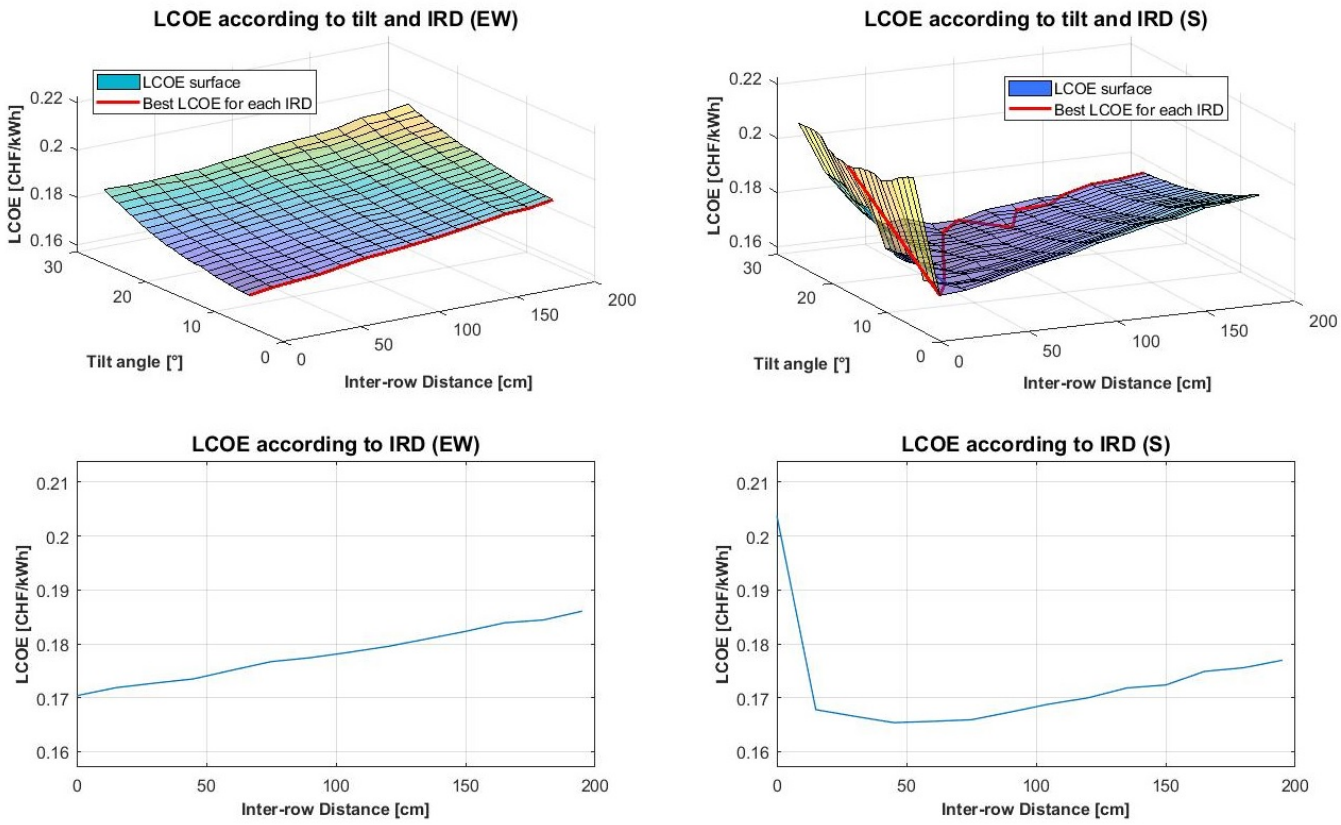


FIGURE 19 – Result of the LCOE indicator for the Garage

At first glance, the graphs above illustrate three main results. First, apart from the shaded zone of S results, the LCOE is increasing with IRD, which significates that the costs are lower for a dense installation, easily explained by the economies of scale (see fig. 16). Secondly, the south-oriented installation has a lower cost of production in comparison to the EW one. This is due to the best angle of irradiation offered by south oriented panels compared to east-west ones, which triggers a higher production per panels despite a slightly smaller number of panels as shown in figure 20. Finally, in the top left graph, it is notable that the optimum line of LCOE for EW is always for 5° tilt regardless IRD. Indeed, as the panels get tilted, the increase their shading effect on each other and decrease the overall performance of the installation, resulting in a higher cost.

For each building, the minimum LCOE has been recorded as well as the main parameters related. Those results are grouped in figure 20.

| | Garage | | Building | | House | |
|---|---|---|---|---|---|---|
| Orientation | S | EW | S | EW | S | EW |
| **LCOE Minimum [Chf/kWh]** | **0.165** | **0.170** | **0.149** | **0.153** | **0.186** | **0.185** |
| Tilt angle [°] | 14 | 5 | 14 | 6 | 5 | 5 |
| Inter-row Distance [cm] | 45 | 0 | 45 | 0 | 15 | 0 |
| Power installed [kWp] | 51.1 | 72.5 | 55.2 | 82.5 | 18.6 | 21.4 |
| Electrical production [MWh/y] | 40.7 | 53.8 | 48.2 | 67.4 | 15.6 | 17.6 |
| Panel production [kWh/panel/y] | 275 | 256 | 301 | 282 | 288 | 283 |

FIGURE 20 – Optimum for each building, orientation and parameters related

The table presented in fig. 20 illustrates well the economies of scale between each roof. Indeed, Building which has the bigger roof has the lowest cost, and House which has the smaller one has the higher costs per kWh produced. The interesting aspect of this cost study is the trade-off between increasing the number of panels for lower installation costs or increasing the distance between them for higher productivity of the panels. In both orientation, a trend goes towards big installations for a low LCOE, showing that the increase of productivity is lower than the decrease of installation cost.

For the House, the difference is really small and the best orientation is East-West. In this case, the roof is smaller and the power installed is more important than the production per panel. For little installations an EW orientation is more adequate as it allows to install more panels without decreasing the production per panel compared to South orientation. It is interesting to see in the table that the small House is the only building to have an optimum cost in S that is for very close panels. This is because all small installations have a strong incentive to install as much panels as possible (see graph 16), which pushes the S optimum to a very small IRD, leading to shading effects which are avoided in an EW installation. As a result, for small flat roofs, EW seems to have lower LCOE than S, and for big flat roofs, S has a lower LCOE than EW.

### 4.1.2 Results for NPV indicator

As a reminder, the NPV indicator represents the discounted value of the cash flows of the project. The advantage of this indicator is that it takes into account all the economic context of the project (installation cost, tariffs, price of electricity, overproduction of electricity, self-consumption, subsidies...). This rich indicator allows to establish a wider evaluation of the project than the LCOE, but it is also more depending on the so-called economic and political context. The result of the Garage for the two different orientation is illustrated in the figure 24. The eq. 8 shows that the returns should increase with self-consumption which itself decreases with the size of the installation. As a result, we can expect a trend of the revenue to incite for smaller installations. In the other hand, the initial investment is inciting to have a big installation because of subsidies and diminishing cost of installation.

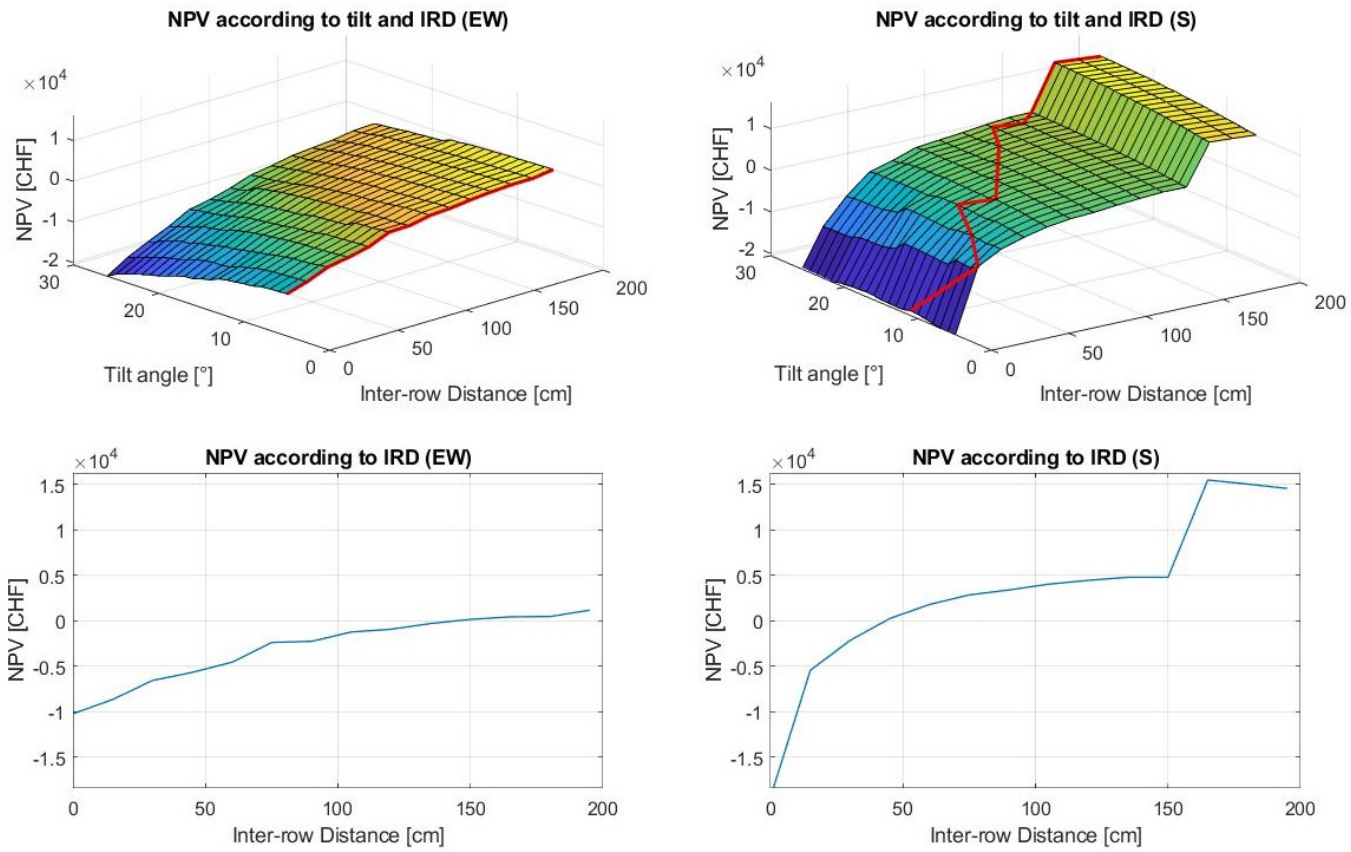


FIGURE 21 – Result of the NPV indicator for the Garage

The graphs of NPV for the Garage shown in fig. 21 add two new considerations to the LCOE analysis. First, we can see that this indicator decreases with the size of installation. This is mainly due to the self-consumption incitation to install few panels (see last paragraph of part 3.3.2). Secondly, we see a direct jump from 5000 CHF to more 15000 CHF on the right part of the S graph. This is due to the change of size of the installation below 30 kWp and the corresponding jump of the tariff at the corresponding value of IRD. Since the EW installation always has a higher density of panels installed than S, we couldn't show this phenomenon for EW in the limit of our parameters.

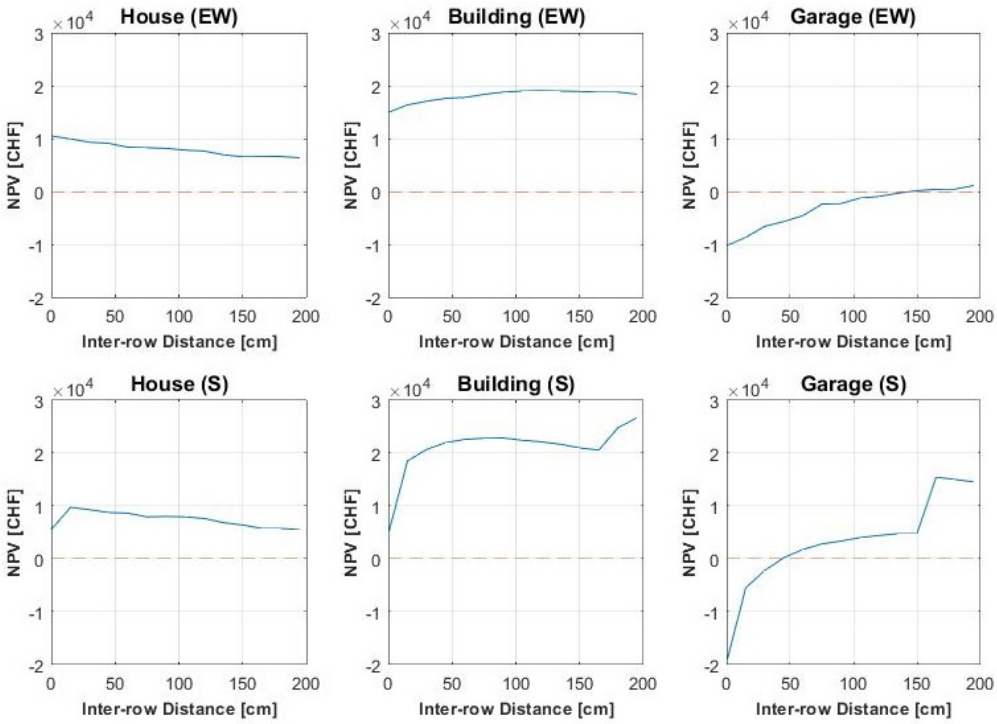


FIGURE 22 – NPV for each building

On fig. 22, we can see that all the buildings are not sensible to the same incentive. The global trend is that Garage and Building follow well the self-consumption rule of privileging small size, whereas House stays too much influenced by the rule of scale to which all small installations are sensitive. The subsidies also incite to increase the size of the installation.

For each building, the maximum NPV has been recorded as well as the main parameters related. Those results are grouped in figure 23. As for the LCOE indicator, the House optimum isn't with a south orientation but an EW orientation due to the small area of the roof.

| | Garage | | Building | | House | |
|---|---|---|---|---|---|---|
| Orientation | S | EW | S | EW | S | EW |
| **NPV [CHF]** | **15476** | **1161** | **26734** | **19079** | **9756** | **10521** |
| Tilt angle [°] | 26 | 5 | 26 | 5 | 5 | 7 |
| Inter-row Distance [cm] | 165 | 195 | 195 | 80 | 15 | 0 |
| Power installed [kWp] | 29.0 | 36.9 | 27.6 | 51.1 | 18.6 | 21.7 |
| Electrical production [MWh/y] | 24.1 | 27.6 | 25.2 | 41.9 | 15.6 | 17.8 |
| Panel production [kWh/panel/y] | 287 | 258 | 315 | 283 | 288 | 283 |

FIGURE 23 – Optimum for each building, orientation and parameters related

### 4.1.3 Results for $CO_2$ indicator

Let's remind briefly the two factors that have an impact on $CO_2$ emissions avoided. First, it will increase with the energy produced (we substitute more German electricity), and it will decrease with the number of panels installed (carbon emissions due to production and installation of each panel). Let's analyze the influence of both factors on the Garage shown in figure 24.

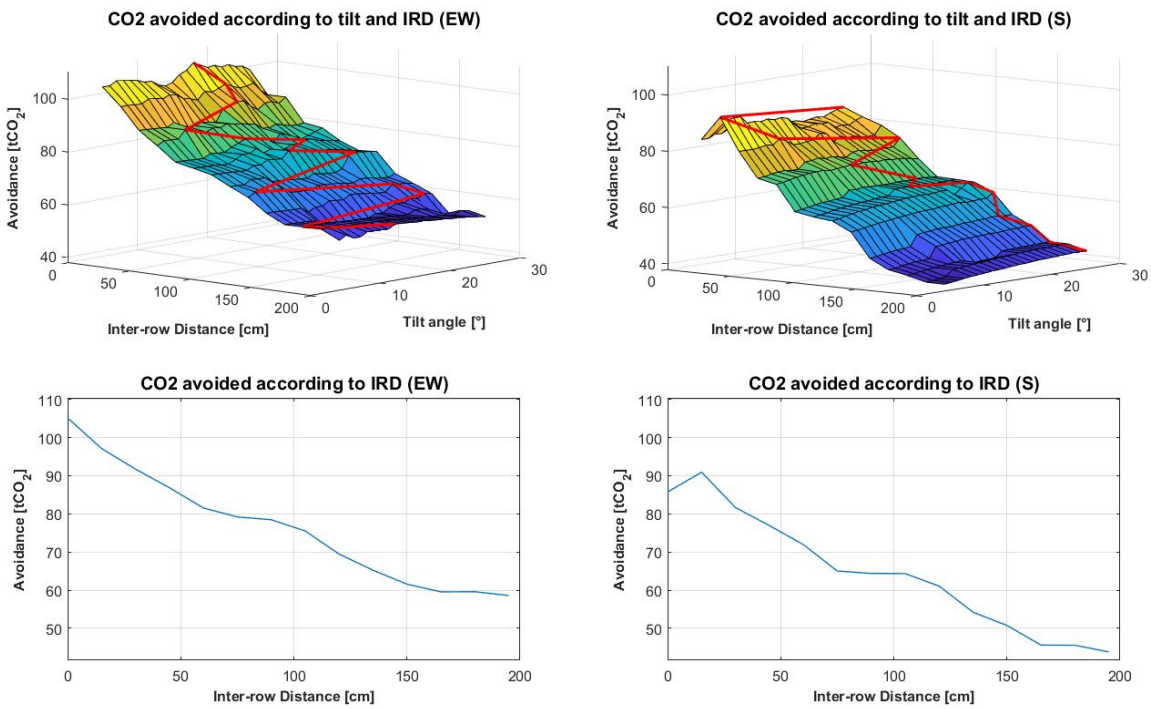


FIGURE 24 – Result of the $CO_2$ indicator for the Garage

It appears clearly on these graphs that carbon savings increase with the size of the installation. This is due to the clearly lower carbon intensity of our panels (around 70 gCO2/kWh) compared to the substituted German mix (estimated to 300 gCO2/kWh in part 3.3.3). This factor is consequently predominant over the number of panels.

For each building, the maximum $CO_2$ avoidance has been recorded as well as the main parameters related. Those results are grouped in figure 25.

| | Garage | | Building | | House | |
|---|---|---|---|---|---|---|
| Orientation | S | EW | S | EW | S | EW |
| **$CO_2$ avoidance [$tCO_2$]** | **276** | **304** | **276** | **395** | **91** | **105** |
| Tilt angle [°] | 5 | 14 | 5 | 5 | 5 | 18 |
| Inter-row Distance [cm] | 15 | 0 | 15 | 0 | 15 | 0 |
| Power installed [kWp] | 63.5 | 75.2 | 70.0 | 83.1 | 18.6 | 23.5 |
| Electrical production [MWh/y] | 48.5 | 54.4 | 58.8 | 67.9 | 15.6 | 18.3 |
| Panel production [kWh/panel/y] | 264 | 249 | 289 | 282 | 288 | 270 |

FIGURE 25 – Maximum avoidance for each building, orientation and parameters related

For each roof the best orientation is the EW, because it allows to install more panels without increasing the problem of shading.

### 4.1.4 Results for Normalized Weighted indicator (NWI)

Now that each individual indicator has been measured and analyzed, a relevant economical-environmental approach of the problem should study both indicators at the same time. It has been chosen that the two studied indicators would be NPV and $CO_2$ for their complementarity and crucial importance in present context. The first step of this analysis is to plot both indicators on the same surface. On the graph below, we have represented the avoided $CO_2$ on the z axis, and the color is for the NPV.

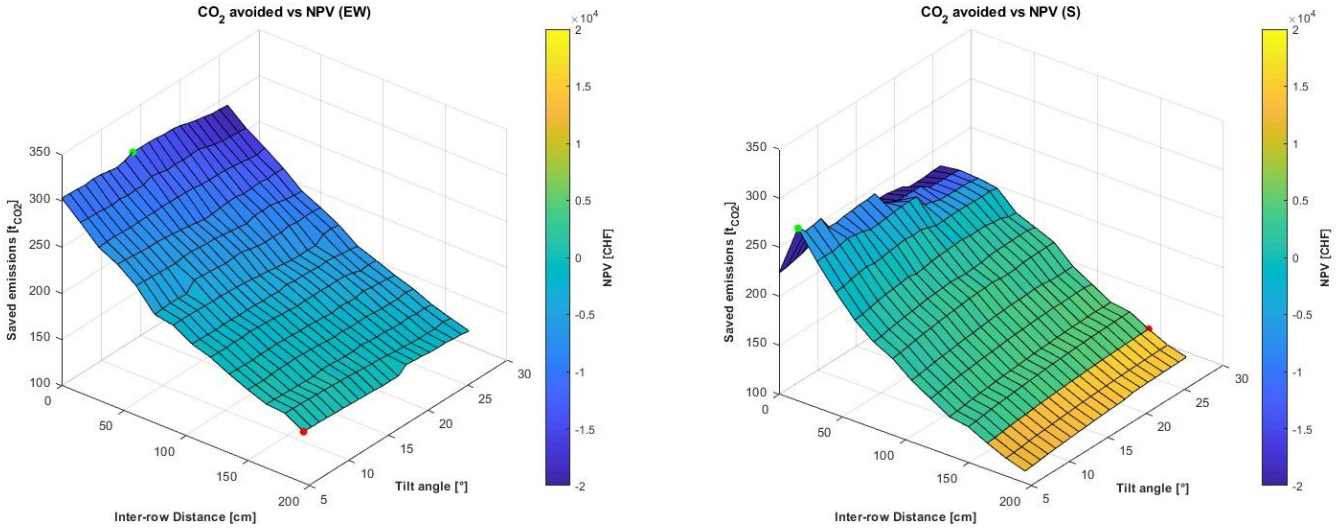


FIGURE 26 – CO2 and NPV optima for the Garage

On the graphs above, the red dot shows the NPV optimum and the green one shows the environmental optimum. It is clear that a trade-off is necessary for the investor who will take the project. Should he maximize the carbon avoided and thus install a lot of panels or should he maximize the profit and follow the rule of small size for a higher self-consumption rate ? To answer this question, one last indicator is introduced : the Normalized Weighted Indicator. As explained in part 3.3.4, this indicator is combining both normalized NPV and normalized $CO_2$ avoided and equally weighting their contribution. Fig. 27 below shows this weighted evaluation for the Garage, enabling a compromising approach of a multilateral problem.

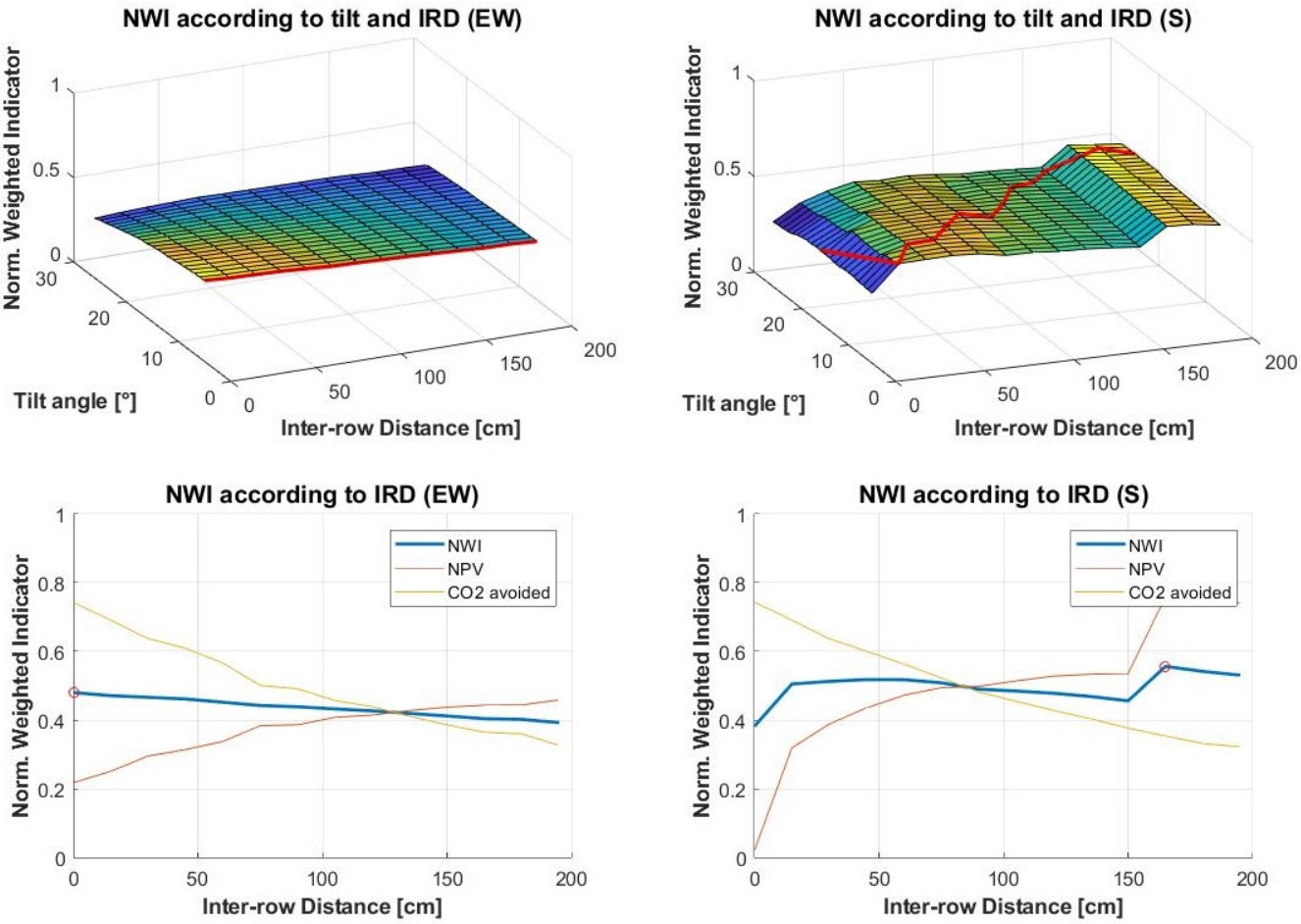


FIGURE 27 – Result of the NWI indicator for the Garage

It is interesting to notice how the NWI allowed to pass from two hilly indicators to a flat and uniform one. The limit of our approach is however the fixed weights of NPV and environment which leads in the EW case to a weighted optimum when the profits are highly negative. This shows how subjective the choice of the weights is. However, thanks to the confrontation of EW to S, we should choose the orientation that leads to the higher NWI, which here is the S with an IRD of 165cm between the panels allowing interesting values of revenues without sacrificing too much environmental performance. This optimum is due to the preferential tariff of electricity below 30kWp. The global stability of the NWI also shows that there is not one specific optimum, and some constraints such as profit>0 could be added.

The 2D curve of maximum NWI per Inter-row Distance is shown for the Building and the House in figures 28 and 29.

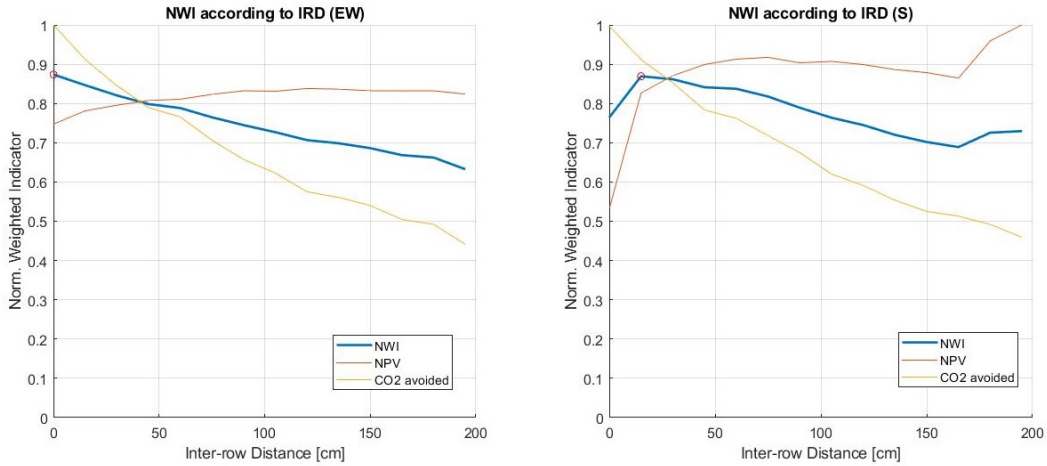


FIGURE 28 – Result of the NWI indicator for the Building

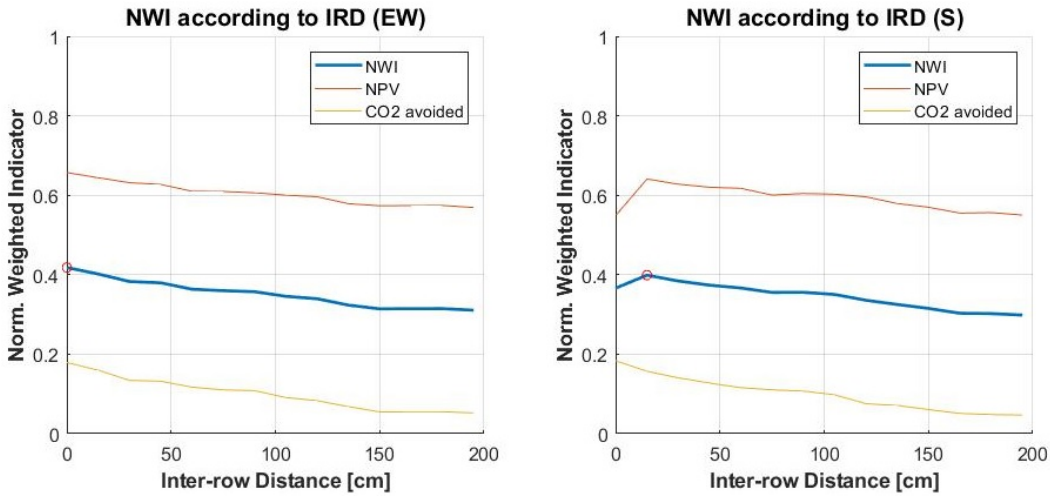


FIGURE 29 – Result of the NWI indicator for the House

The NWI is very good to compare the level of impact of two projects. Indeed, comparing fig.28 to fig.29 shows a ratio close to 2 between the overall performance of the Building and that of the House. This shows how the potential of the building is bigger than the one of the House both environmentally and economically. The optimum is in both case at a very high level of CO2 avoided even in the case of Building where the profit is not maximized at the optimum NWI. To have the biggest impact, this result shows that it is important to develop PV installation on the biggest roofs in a first time.

For each building, the NWI optimum has been recorded as well as the main parameters related. Those results are grouped in figure 30.

| | Garage | | Building | | House | |
|---|---|---|---|---|---|---|
| Orientation | S | EW | S | EW | S | EW |
| **NWI [-]** | **0.56** | **0.48** | **0.869** | **0.874** | **0.40** | **0.42** |
| Tilt angle [°] | 23 | 5 | 5 | 5 | 5 | 7 |
| Inter-row Distance [cm] | 165 | 0 | 15 | 0 | 15 | 0 |
| Power installed [kWp] | 29.0 | 72.5 | 70.0 | 83.1 | 18.6 | 21.7 |
| Electrical production [MWh/y] | 24.0 | 53.8 | 58.8 | 67.9 | 15.6 | 17.8 |
| Panel production [kWh/panel/y] | 286 | 256 | 289 | 282 | 288 | 283 |

FIGURE 30 – Maximum NWI for each building, orientation and parameters related

To conclude this part, the optimal arrangements selected for the three roofs are the following :

| | Tilt | IRD | Orientation |
|---|---|---|---|
| House | 7 | 0 | EW |
| Garage | 23 | 165 | S |
| Building | 5 | 0 | EW |

TABLE 3 – Result of the NWI indicator for the House

### 4.1.5 Recap : comparison between indicators

The table 4 shows the power installed corresponding to the optimal indicators (between the two orientation) of each house and it also shows the maximal possible installed power for each roof (right column) according to the variable parameters. The table 5 shows the percentage of the maximal for each kWp of optimal indicator. This allows to highlight the different trends between the indicators.

| | **Power installed [kWp]** | | | | |
|---|---|---|---|---|---|
| **Indicator** | **LCOE** | **NPV** | **CO2** | **NWI** | **MAX** |
| **Garage** | 51.1 | 29.0 | 75.2 | 29.0 | **76.2** |
| **Building** | 55.2 | 27.6 | 83.1 | 67.9 | **93.5** |
| **House** | 21.4 | 21.7 | 23.5 | 21.7 | **23.5** |

TABLE 4 – Power installed for each optimal indicator and maximum power possible

| | **Percentage of Size max [%]** | | | |
|---|---|---|---|---|
| **Indicator** | **LCOE** | **NPV** | **CO2** | **NWI** |
| **Garage** | 67 | 38 | 99 | 38 |
| **Building** | 59 | 30 | 89 | 73 |
| **House** | 91 | 92 | 100 | 92 |

TABLE 5 – Percentage of power installed of the optimal indicators to the maximal

The LCOE indicator prefers big installation, but not too big in order to conserve a good trade-off between the power installed and the production per panel as seen in chapter 4.1.1.

The NPV indicator aims for installation below 30 kWp, as the feed-in tariff is higher. In this case, all buildings seem to converge to the same range of installed power even if the roofs are quite different.

The $CO_2$ indicator increases as the production of electricity is increasing. That is why this indicator aims for the biggest power installed on each roof, as seen in chapter 4.1.3.

The NWI indicator a mixed of the NPV and CO2 indicator and follows both trend of those previous indicators.

## 4.2 Advanced scenarios and comparison to horizontal ones

This part focus on finding a linear relation between a horizontal estimation of an installation potential (see section 3.2.2) and a more realistic advanced estimation. The main purpose of this step is to provide a simple tool to go from quick horizontal estimation to more advanced and realistic estimation.

As seen in part 4.1.4, we have seen that NWI is a compromising indicator allowing a multilateral assessment of the potential of a roof. However, this indicator also has drawback such as the subjective choice of weights and of normalization, and a final choice proposing only one trade-off which is not very representative of one specific profile of investor. For this reason, we have chosen to realize four different scenarios, one per indicator, in which we compare an optimal arrangement to the horizontal

one. The three first indicators are applicable in specific situations, the last one which is a mix of previous indicators is more representative of a global system where investors with different interests would evolve.

### 4.2.1 Industrial scenario

In the industrial scenario, the LCOE indicator is used. In reality it could be the case for an electricity company, distributor or producer, indirectly the property of the Canton/State, that doesn't touch fees deduction and doesn't take into account the subsidies. The LCOE advanced potential estimation in Table 6 comes from the results shown in Fig. 20

| | **Horizontal production [MWh/yr]** | | | | |
|---|---|---|---|---|---|
| | **Aligned** | **South** | **Stairwell** | **Chimneys** | **LCOE** |
| **Garage** | 67.8 | 54.8 | 54.8 | 54.8 | **40.7** |
| **Building** | 91.3 | 74.9 | 73.3 | 66.0 | **48.2** |
| **House** | 27.7 | 22.8 | 20.3 | 19.0 | **17.6** |

Table 6 – Comparison of horizontal scenario of production with best LCOE production

| | **Variation** | | | |
|---|---|---|---|---|
| | **Aligned** | **South** | **Stairwell** | **Chimneys** |
| **Garage** | 1.67 | 1.35 | 1.35 | 1.35 |
| **Building** | 1.90 | 1.55 | 1.52 | 1.37 |
| **House** | 1.57 | 1.29 | 1.16 | 1.08 |
| **Mean ratio** | **1.71** | **1.40** | **1.34** | **1.26** |
| **STD** | **0.16** | **0.14** | **0.18** | **0.16** |

Table 7 – Ratio of the horizontal production over the tilted one

Example of table use : If a company uses the 'Aligned' simplified model to evaluate the potential of a project, and the model forecasts a production of 35 MWh/yr, then it should divide it by the 'Mean ratio' of 1.71 to reach our advanced estimation for a project realized by industrial actors prioritizing the LCOE. In this example, 20.5 MWh/yr.

### 4.2.2 Private installer scenario

In the private installer scenario, we suppose the stakeholder to be a private investor looking for profit, touching subsidies and deduction fees. The investor would generally be the owner or co-owner of a building with a flat roof.

| | **Horizontal production [MWh/yr]** | | | | |
|---|---|---|---|---|---|
| | **Aligned** | **South** | **Stairwell** | **Chimneys** | **NPV** |
| **Garage** | 67.8 | 54.8 | 54.8 | 54.8 | **24.1** |
| **Building** | 91.3 | 74.9 | 73.3 | 66.0 | **25.2** |
| **House** | 27.7 | 22.8 | 20.3 | 19.0 | **17.8** |

Table 8 – Comparison of horizontal scenario of production with best NPV production

| | Variation | | | |
|---|---|---|---|---|
| | **Aligned** | **South** | **Stairwell** | **Chimneys** |
| **Garage** | 2.81 | 2.28 | 2.28 | 2.28 |
| **Building** | 3.62 | 2.97 | 2.91 | 2.62 |
| **House** | 1.55 | 1.28 | 1.14 | 1.07 |
| **Mean ratio** | **2.66** | **2.18** | **2.11** | **1.99** |
| **STD** | **1.05** | **0.85** | **0.89** | **0.82** |

TABLE 9 – Ratio of the horizontal production over the tilted one

In this scenario, the ratio of variation would be around 2 for a detailed horizontal model.

### 4.2.3 Ecologist installer scenario

This scenario is aimed at establishing a link between horizontal estimations from simplified models and an advanced estimation where the stakeholder is only according interest to CO2 avoided. If we imagine that the price of carbon tax increases, then this scenario should become more representative of investors.

| | Horizontal production [MWh/yr] | | | | |
|---|---|---|---|---|---|
| | **Aligned** | **South** | **Stairwell** | **Chimneys** | **CO2** |
| **Garage** | 67.8 | 54.8 | 54.8 | 54.8 | **54.4** |
| **Building** | 91.3 | 74.9 | 73.3 | 66.0 | **67.9** |
| **House** | 27.7 | 22.8 | 20.3 | 19.0 | **18.3** |

TABLE 10 – Comparison of horizontal scenario of production with best $CO_2$ production

| | Variation | | | |
|---|---|---|---|---|
| | **Aligned** | **South** | **Stairwell** | **Chimneys** |
| **Garage** | 1.25 | 1.01 | 1.01 | 1.01 |
| **Building** | 1.35 | 1.10 | 1.08 | 0.97 |
| **House** | 1.51 | 1.24 | 1.11 | 1.04 |
| **Mean ratio** | **1.37** | **1.12** | **1.07** | **1.01** |
| **STD** | **0.13** | **0.12** | **0.05** | **0.03** |

TABLE 11 – Ratio of the horizontal production over the tilted one

As the $CO_2$ indicator aims to put as much panels as possible, the variation between the horizontal scenarios and the ecologist scenario is really little. For each building, the production of this scenario is nearly the same as the horizontal one.

### 4.2.4 Mixed scenario

In this scenario, we don't focus strictly on one profile of investor but more on a cluster of economic and environmental actors resulting in an averaged mix of different personal interests. The indicator followed in this part is the NWI.

| | Horizontal production [MWh/yr] | | | | |
|---|---|---|---|---|---|
| | **Aligned** | **South** | **Stairwell** | **Chimneys** | **NWI** |
| **Garage** | 67.8 | 54.8 | 54.8 | 54.8 | **24.0** |
| **Building** | 91.3 | 74.9 | 73.3 | 66.0 | **67.9** |
| **House** | 27.7 | 22.8 | 20.3 | 19.0 | **17.8** |

TABLE 12 – Comparison of horizontal scenario of production with best NWI production

| | Variation | | | |
|---|---|---|---|---|
| | **Aligned** | **South** | **Stairwell** | **Chimneys** |
| **Garage** | 2.83 | 2.28 | 2.28 | 2.28 |
| **Building** | 1.35 | 1.10 | 1.08 | 0.97 |
| **House** | 1.55 | 1.28 | 1.14 | 1.07 |
| **Mean ratio** | **1.91** | **1.56** | **1.50** | **1.44** |
| **STD** | **0.80** | **0.64** | **0.68** | **0.73** |

Table 13 – Ratio of the horizontal production over the tilted one

In this mixed scenario, the variation depends a lot of the building, but the mean variation still lower than 2 for each horizontal scenario.

### 4.2.5 Synthesis of the comparison

Since the two scenarios Aligned with building and South oriented are quite easy to simulate, it is interesting to assess which one of them is leading to ratios close to 1 and with a low STD. Without surprise, the South scenario always proposes ratios closer to 1 in comparison to the Aligned scenario. This is linked to the south orientation of our advanced scenarios. Moreover, the STD is always lower with the South oriented approach. Indeed, the South model is necessarily leading to ratios closer to 1 than the Aligned model, where the ratios can be very volatile between 1 and 3. To conclude, the South oriented scenario leads to estimations of potential that are closer to the advanced ones and with a lower volatility, compared to the ones of the Aligned scenario.

# 5 Discussion

## 5.1 Sensibility on the optimum indicators

In the chapter 4, an optimum has been found for each indicator and each building. However, those optima can be really sensible to little variation of parameters. The only indicator optimum which isn't very sensitive is the $CO_2$ emissions. In the economic indicators (LCOE and NPV), the optimum can vary a lot according to small changes as shown in following statements. The subsidies, the tariffs and the price of electricity are contributing to the influence of self-consumption on the optimum. The discount rate has an increasing influence with the time, which means that a decrease of this rate would trigger a higher importance of the future entries. This would decrease the influence of subsidies and installation cost and increase the influence of the cost of electricity and self-consumption.

For all these reasons, the optimum value might undergo some variations. However, such variations impact the size of the installation itself. The graph 31 shows a relevant phenomenon concerning sensibility of the installation size to a +5% variation of the LCOE optimum. The variation of 5% induces a change of more than 65% and 67% of the power installed for the S and EW orientation respectively. It why in the case of an electricity retailer or private PV installer, many possibilities still great around the optimum.

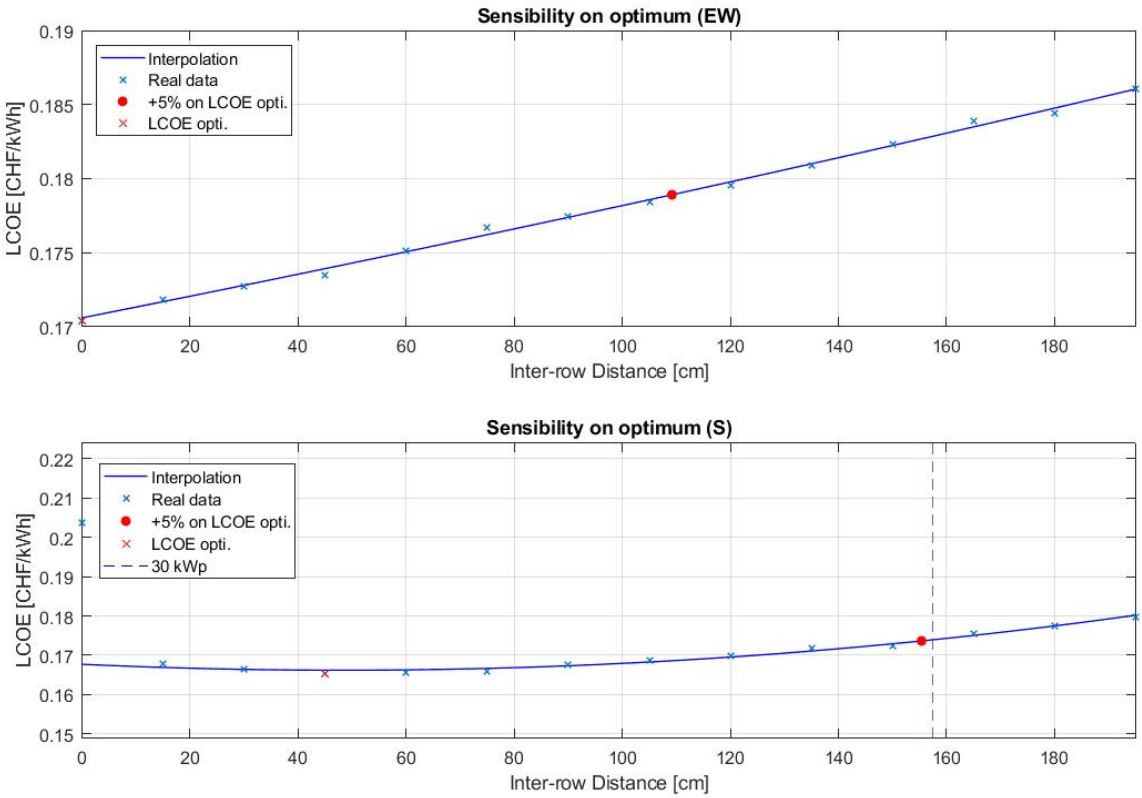


FIGURE 31 – Sensibility to optimum variation of installation size (Garage roof)

## 5.2 Influence of context within a building

The influence of the context has been studied for each orientation of each building. The result is presented with box-plots in the figure 32. The parameter statistically studied in each case is the variation of each parametric point between the production matrix with context and without context.

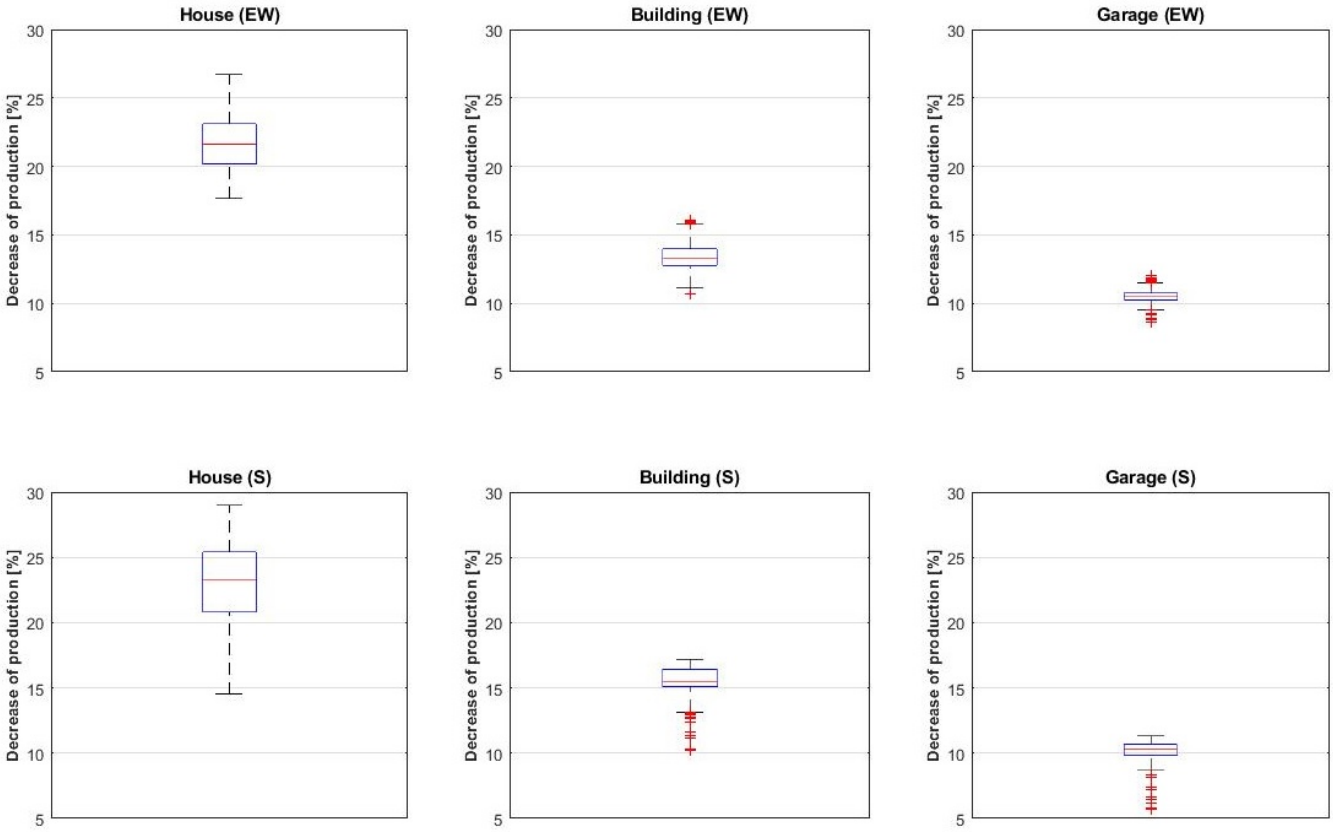


FIGURE 32 – Box-plots of the context influence on the production

On each roof, the context (surrounding buildings and roof obstacles) decreases the overall production for each parametric point. In the House, the decrease is the more important (around 23%) as the proportion of obstacles (chimneys, stairwell) per area of roof is the very important. It is also the high proportion that explains why the variation is more dispersed than in the two others roofs. In the Building, this proportion of obstacles is lower, as well as the decrease of production (medians around 13 and 16 %). The Garage is less impacted by the context with a median decrease of around 10.5%. Our values come to confirm those of Takebayashi [18] estimating the influence of the surrounding context on production between 14 and 21% in Osaka.

With House and Building in South orientation, the decrease in production is slightly higher than with EW orientation. This effect is maybe due to the automatic disposal of panels during the parametric simulation ; with a south orientation with high IRD, panels with south orientation are more susceptible to be close to an obstacles and so shadow.

Finally, even if the garage is the lowest and could be more impacted by the context of the surrounding building, we see that the obstacles on roof are more likely to decrease the production.

## 5.3 Influence of by-pass

In chapter 3.2.4, we explain that a panel with bypass diodes is simulated in the parametric simulation. This is done partly with the help of 4 sensors on the panel. At the beginning of the project, only one vector was used and it was positioned on the panel bottom. The figure 33 shows the difference of the best production per IRD in function of the number of sensors. The best tilt angle according to this production is also showed. The result shown represents the south orientation of the Garage.

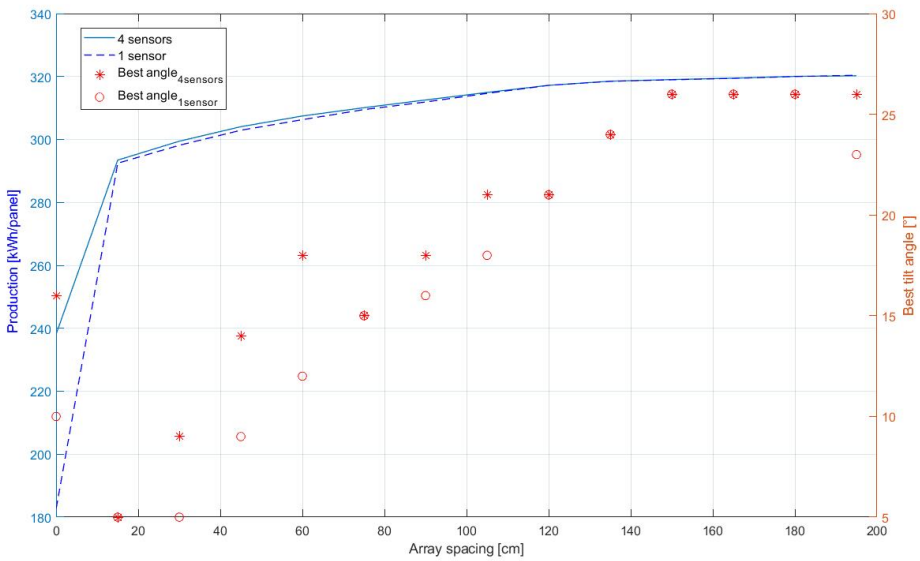


FIGURE 33 – Difference of production in function of panel sensor number

This shows that with 4 sensors the production is better when the panels are close but the difference is really small after 1m of IRD. The higher production below 1m is due to the higher tilt angle of the panels. Indeed, even if one part of the panel is shaded sometimes with higher tilt, the by-pass system (4 sensors) allows a high production.

For EW orientation, the effect of the 4 sensors is less important as the panels are less impacted by shading.

## 5.4 Limitations

Several points have been neglected during the project or could be improved. They are discussed in this section.

During the parametric simulations, we assume that tilt between 5° and 26° were big enough to contain all optimal indicators for each roof, orientation and IRD. For the IRD, we assume that all optimal indicators would be between 0 m and 1.95 m. In the chapter 4, we saw that for IRD higher than 1.3 m, 26° is sometimes limiting but only for south orientation. For the NPV indicator, the final optimum of the Garage and Building is at 26° of tilt, but it could higher (around 30° according to in Annexe), increasing a bit the NPV indicator.

We also saw that for the NPV, the IRD limit of 1.95 was not enough for the Garage and the Building. In this case, the results could slightly change as the number of panel installed would decrease with higher IRD and so decrease the total production.

In the parametric simulations, we use a panels with by-pass diodes in order to simulate more precisely the behavior of a real panel. This by-pass system tends to increase the tilt angle of the panels, especially with low IRD (see chapter 5.3). By allowing shading on panels during some part of the year, an effect has been neglected. As explained in the literature [28], shading speeds up the degradation process creating differences of voltage inside the panel PV cells. If this effect is proved, this could induce a more spaced design of the installation which avoids shading.

In all indicators, a constant production of panel through their lifetime has been assumed. Even if we account of the degradation of the panels, we take the mean efficiency over the lifetime and did not assume take into account the variation of this efficiency. In our case, the efficiency is lower at the beginning of the panels life and higher at the end.

In the parametric simulations of South orientation, the panels were directed to the south (azimuth of 0°), assuming that it is the most productive azimuth. In fact, the azimuth could be better according to local meteorological trends [8] and could be tested. For example, it is possible that the presence of fog in the morning favors an azimuth to the west.

The performance ratio of the panel is assumed to be constant for each parametric simulation. This is wrong as the effect of the temperature will be more important in summer and on panel with a low tilt. At the beginning, we wanted to take into account this effect, but finally it has not been possible due the choice of by-passed panel and the presence of 4 sensors per panel. Furthermore, this performance ratio could also be better for more tilted panel which are less impacted by soil, leafs and snow deposition.

The use of normalization following Steubing's approach [34] for estimating a weighted indicator presents some limitations as discussed several times in this report. Indeed, the mark 0 is given for the lower value of each indicator and 1 for the higher, but in our case the minimum NPV is highly undesirable whereas the minimum CO2 avoided is very acceptable, so putting them equally to 0 doesn't seem very fair for the environmental factor. The problem is that all investors are different and establishing an optimal weighting to illustrate their interests is beyond the scope of this study.

## 5.5 Outlook

To go further in this project, three different things could be done.

First, more roof should be studied with the defined indicators. The size of the roof is one of the main criterion to estimate is behavior within the different indicators. The effect of this area could be studied through procedural modeling in order to have a relevant set of data.

Second, the limits of the tilt angle and inter-row distance should be increased in the parametric simulations. We have seen that sometimes, the limits aren't big enough and the optimum could be different and higher. If we should redo the parametric simulations, an upper limit of 32° for the tilt angle would be taken and the IRD upper limit of the Garage and the Building would be risen to 6 meters (but with 0.5m of interval).

Third, the azimuth of the south orientation should be studied more in detail. As discussed before, it is possible that other azimuths, close to the south increase the production due to local meteorologic trends at certain time of the day.

# 6 Conclusion

Current studies of solar potential estimation on flat roofs are able to provide always more precise results with 3D or 2D models. However, the link between simplified 2D models and advanced 3D models stays imprecise and leads to the use of various performance factors that are only approximations. Furthermore, classical scenarios for urban-scale approach whether consider a horizontal approach or follow a simplified fixed rule for the arrangement of solar arrays on flat roofs. This report proposes to take into consideration a set of parameters and indicators in order to evaluate for each roof the best arrangement, and deduce the solar potential from this contextual consideration. An evaluation of both EW and S orientation is also realized.

The methodology proposed consists of a model for evaluating different horizontal and advanced scenarios in order to finally establish a relation between them. The advanced scenarios result from a parametric study on Grasshopper and its optimization according a set of four key performance indicators. This model was implemented in a case study in Switzerland, where three different roofs were used to test the model under different constraints.

The four studied indicators all led to specific advanced scenarios. Generally, the EW orientation was allowing higher size of installations than the S one, but according to the context and to the indicator, both could be considered as the best orientation. A set of ratios between horizontal and advanced arrangements was deduced from the model.

Finally, this research brings a new point of view on the three following aspects : the choice of best arrangement for solar potential estimation on flat roofs, the comparison between advanced tilted scenarios and different horizontal scenarios as well as the consideration of EW oriented panels. Even though the model has not been confronted to real tests yet, it brings coherent values with Takebayashi [18] in terms of context influence on PV generation. Various improvements remain to be done, especially in terms of number of studied roofs, parameters range and computation time of the overall simulation.

# 7 Aknowledgments

We thank warmly Giuseppe Peronato for his supervision, his valuable guidance, his help for the numerous simulations and skills with the different programs and thanks to Sergi Aguacil for his supervision and precious advices all along the project. We are grateful to the LIPID laboratory for letting us use diverse material and their computation capacity all along the project. Thank you also to Eric Demoingeot, from Viteos, for his availability and his precious advises.

# 8 Used abbreviations

| Abbreviation | Description |
|---|---|
| PV | Photo-Voltaic |
| kWp | Power peak installed in kW |
| IRD | Inter-row Distance |
| EW | East-West orientation |
| S | South orientation |

# 9 Annexes

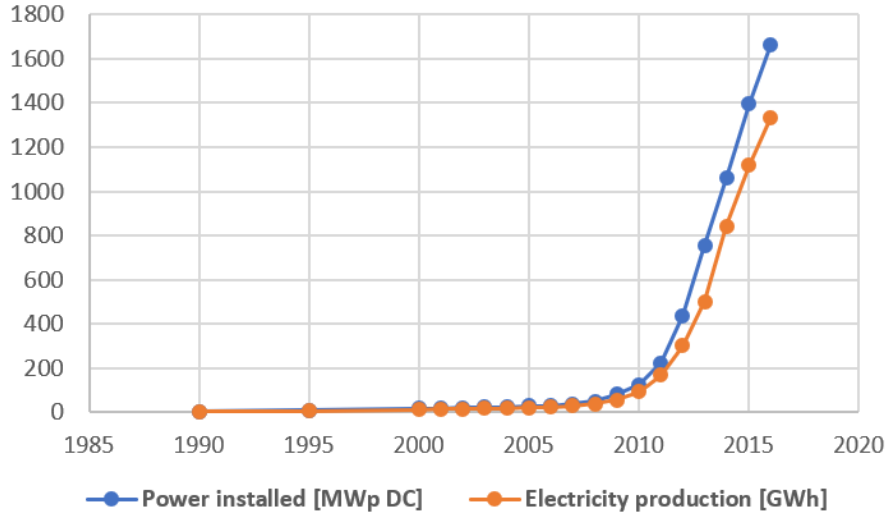


FIGURE 34 – Evolution of Swiss installed power peak and production

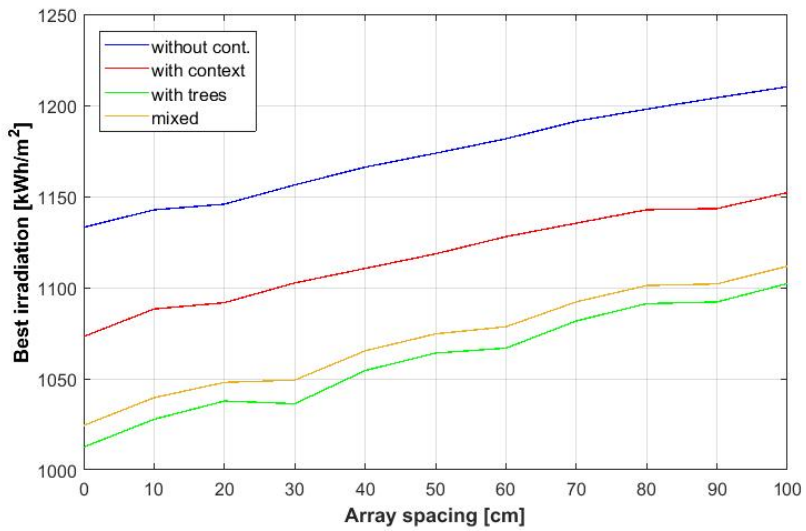


FIGURE 35 – Effect of trees on the total yearly irradiation (for a random set of garage data)

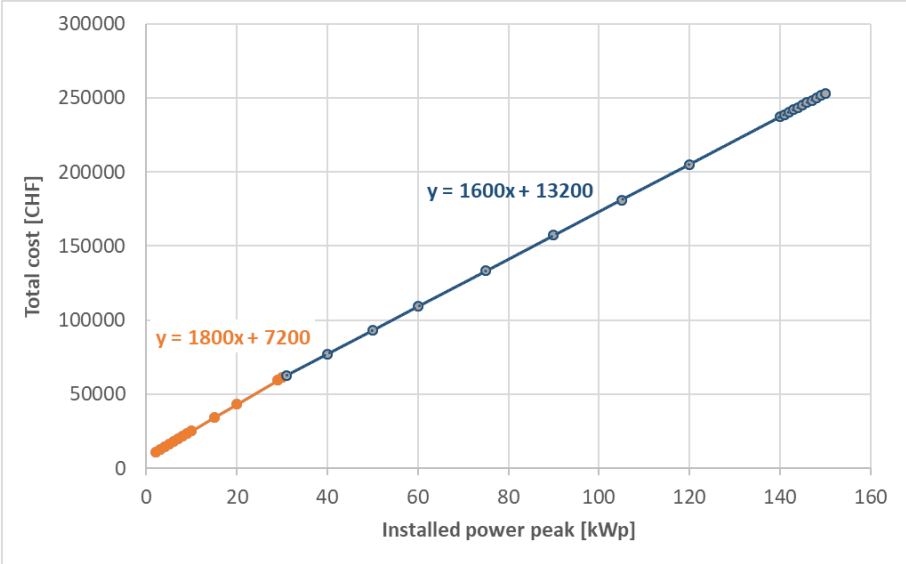


FIGURE 36 – Data used to find the cost in functions of the number of installed panels

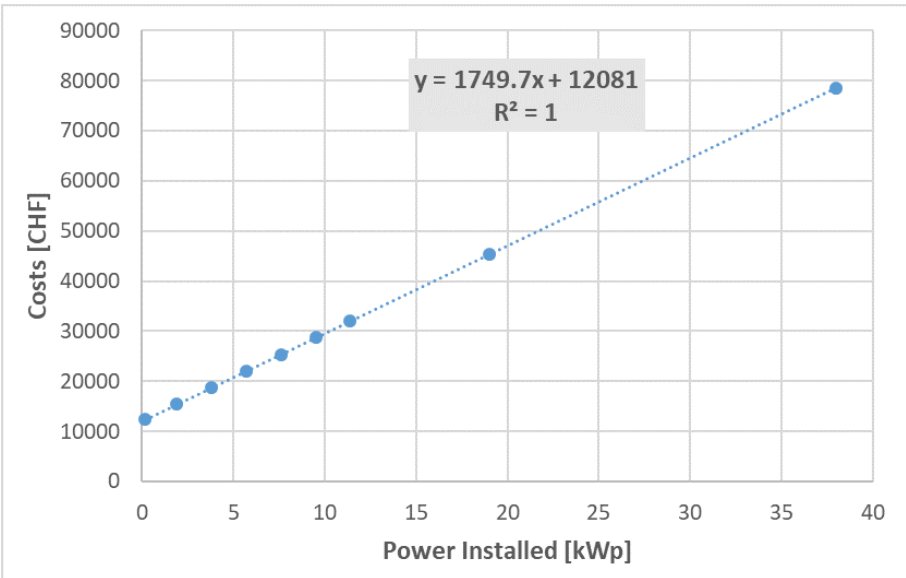


FIGURE 37 – Megaslate price - Cost function of kWp installed

## 9.1 Relation between tilt angle and array spacing - Theoretical approach

### Sun Position

In order to propose a relevant set of scenarios, it is necessary to know the evolution of the sun's position over one day in Neuchâtel. This position is depending on the month, the time and the latitude of the panels location on earth (47° latitude for Neuchâtel). All those informations are available on the interactive map of `sunearthtools.com`.

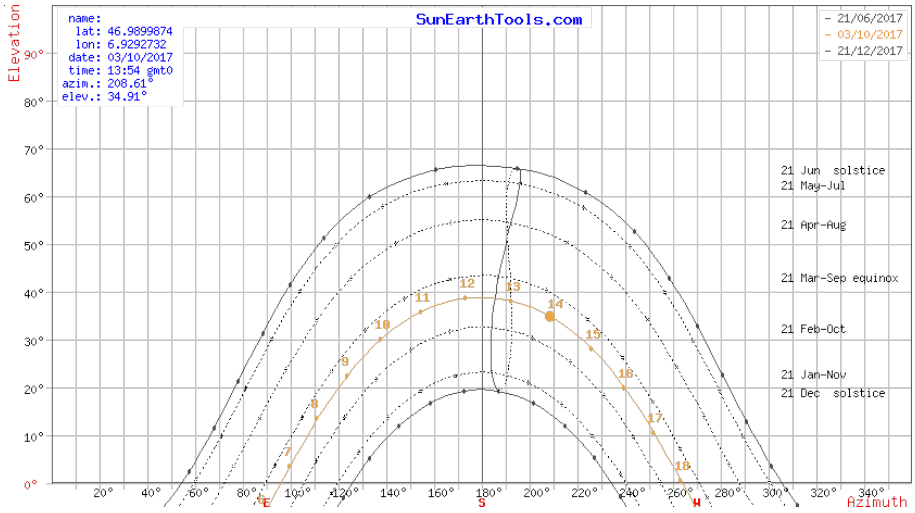


FIGURE 38 – Sun's angular position over the day at each month of the year 2017

This graph provided by SUNEARTHTOOL shows us that the sun's position is symmetric around 12 :30. Therefore, shading effects occur during a symmetric period around 12 :30, which implies that one scenario could be "no shading effects between 11 a.m. and 2 p.m." for example.

Not only this graph provides us pieces of information about the sun's position evolution over over the day, but also over the year, with a symmetry of sun's position appearing around the solstices. As a result, three scenarios seem to be covering the four seasons, because the sun's orientation is the same on spring and on autumn.

In fact, a seasonal study shows that the irradiation in spring is much higher than in autumn. The main explanation is that the weather is sunnier in spring and cloudier in autumn. This shows a limitation of the sun position parameter, and the importance of weather data for solar installation design.

In order to find the best positioning of solar arrays in term of tilt angle and distance between arrays, we start by studying a single solar panel in the Rhino model without any surrounding environment.

### Best angle of one panel

Through the RHINOCEROS interface, the hourly solar irradiation for one solar panel is calculated for each tilt angle. This allow to find the best angle for the yearly cumulative production or seasonal productions. The result of the computation can be seen in fig. 39.

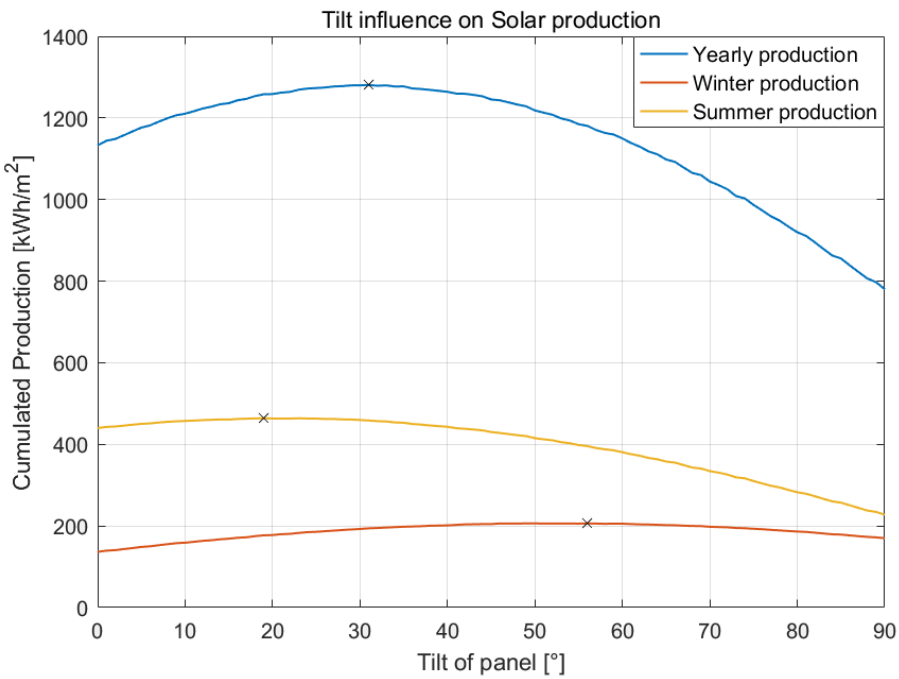


FIGURE 39 – Solar production according to the tilt of the panel

In the figure, for each curve a cross shows the maximum production and related angle. Table 14 resumes the best angle found for each period.

| **Period** | **Best angle [°]** |
|---|---|
| Year | 31 |
| Winter | 56 |
| Summer | 19 |

TABLE 14 – Best angle for each period

### Array spacing

Once the best angle found for the yearly production, we try to define the best distance between solar arrays for this angle. The formula which link the angle and the shadow of a panel is the following [13] :

$$S = \frac{H}{\tan VSA} \tag{9}$$

$$\tan VSA = \frac{\tan \alpha_s}{\cos \gamma_s} \tag{10}$$

$$H = W_p \cdot \sin \beta_a \tag{11}$$

where $S$ is the array spacing, $VSA$ is the vertical shading angle between the sun and the array, $H$ is the height of the tilted module, $W_p$ is the array row width, $\gamma_s$ and $\alpha_s$ are the azimuth (0–360 from North) and altitude angles of the sun and $\beta_a$ is the tilt angle of the PV array relative to the horizontal frame of reference. Figure 40 is a sketch of the different parameters.

From those equations, we calculate the length of the perpendicular shadow for 3 different dates (see fig. 41) in order to see the impact on the solar array. For each of those days, we calculate the hourly length of the shadow. As expected, the biggest shadow is found on the 21$^{\text{th}}$ of December and the smallest on the 21$^{\text{th}}$ of June. The shadow shorten as the sun rise and lengthen as the sun decrease. The minimum length of the shadow is always around 1 p.m.

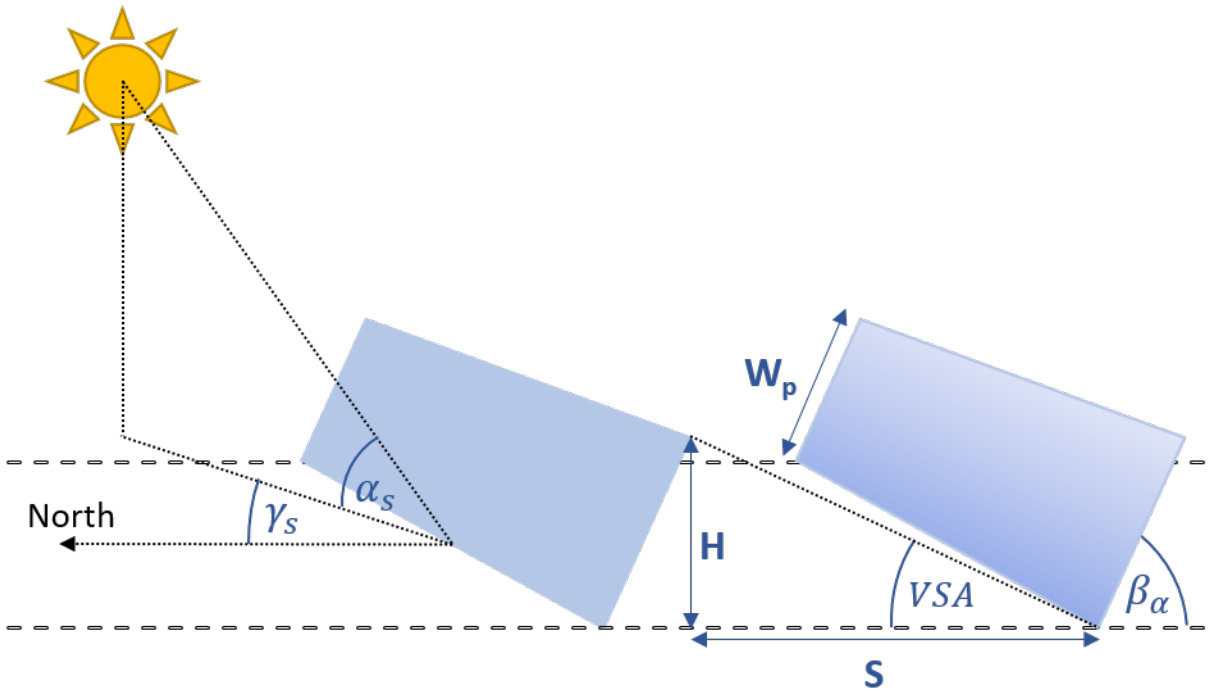


FIGURE 40 – Parameter need to compute the shadow caused by solar panel, based on [13]

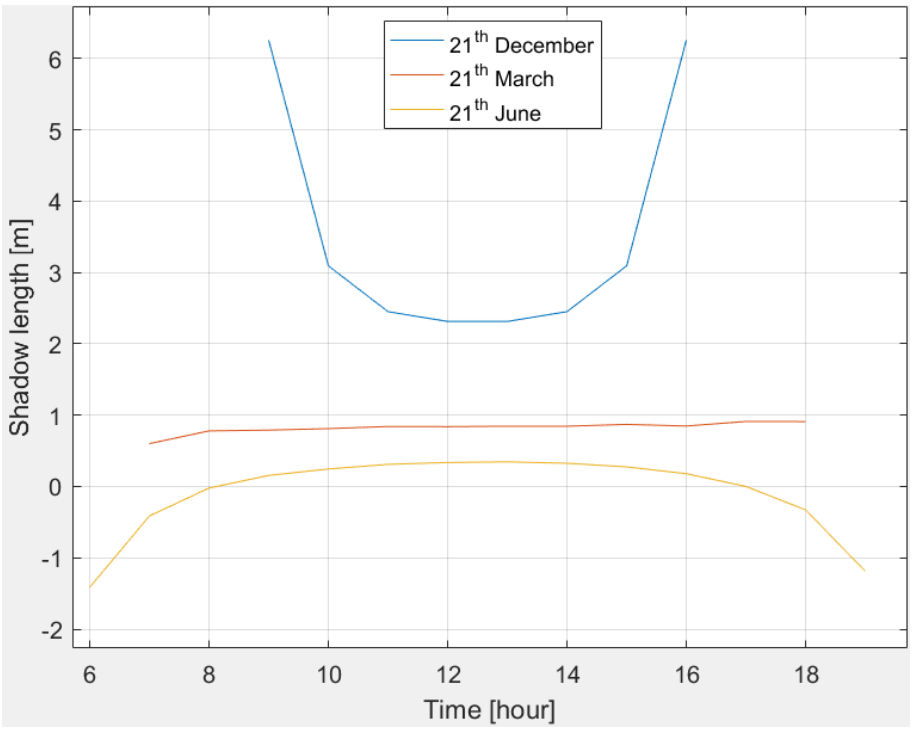


FIGURE 41 – Daily evolution of shadow length

The goal of the theoretical approach is to choice the best distance between arrays to avoid shadow on the solar panels, but the difficulty is to define a time-lapse during which shadows don't get over other panels. For example, a possibility is to decide that during all the year, the panel aren't shadowed between 10 a.m. to 3 p.m. and then to fix the distance between solar arrays. The problem with such a decision may be the loss of production per panel (array more spaced) or the loss in the total production (array more tighten) and the justification of the choice of the time-lapse.

Moreover, this approach neglects the effect of indirect irradiation that occurs in the model. In consequence, the best angle for a solar installation is not the same as for one single panel.

# References


[1] Office Fédérale de l'Energie. Statistique globale suisse de l'énergie 2016, 2016.

[2] International Energy Agency. Potential for Building Integrated Photovoltaics, 2002.

[3] Office fédéral de topographie Office fédéral de l'énergie. Le site www.toitsolaire.ch indique le potentiel des toits des bâtiments en matière d'énergie solaire.

[4] Stade de Suisse | Berne | MyCityHighlight.

[5] Solstis. Solstis le partenaire pour votre centrale solaire photovoltaïque en Suisse romande - EPFL 630 kWc.

[6] C. L. Cheng, Charles S. Sanchez Jimenez, and Meng-Chieh Lee. Research of BIPV optimal tilted angle, use of latitude concept for south orientated plans. *Renewable Energy*, 34(6) :1644–1650, June 2009.

[7] Jayanta Deb Mondol, Yigzaw G. Yohanis, and Brian Norton. The impact of array inclination and orientation on the performance of a grid-connected photovoltaic system. *Renewable Energy*, 32(1) :118–140, January 2007.

[8] Joshua D. Rhodes, Charles R. Upshaw, Wesley J. Cole, Chris L. Holcomb, and Michael E. Webber. A multi-objective assessment of the effect of solar PV array orientation and tilt on energy production and system economics. *Solar Energy*, 108(Supplement C) :28–40, October 2014.

[9] Interview with Eric Demoingeot de Viteos SA, november 2017.

[10] Christian Roecker Maria Cristina Munari Probst. Urban Acceptability of Building Integrated Solar Systems : LESO-QSV Approach. January 2011.

[11] Hussein A. Kazem, Tamer Khatib, K. Sopian, and Wilfried Elmenreich. Performance and feasibility assessment of a 1.4kw roof top grid-connected photovoltaic power system under desertic weather conditions. *Energy and Buildings*, 82(Supplement C) :123–129, October 2014.

[12] Nuria Novas Castellano, José Antonio Gázquez Parra, Juan Valls-Guirado, and Francisco Manzano-Agugliaro. Optimal displacement of photovoltaic array's rows using a novel shading model. *Applied Energy*, 144(Supplement C) :1–9, April 2015.

[13] J. K. Copper, A. B. Sproul, and A. G. Bruce. A method to calculate array spacing and potential system size of photovoltaic arrays in the urban environment using vector analysis. *Applied Energy*, 161(Supplement C) :11–23, January 2016.

[14] C. L. Cheng, C. Y. Chan, and C. L. Chen. Empirical approach to BIPV evaluation of solar irradiation for building applications. *Renewable Energy*, 30(7) :1055–1074, June 2005.

[15] Gui Ning, Li Junnan, Dong Yansong, Qiu Zhifeng, Jia Qingshan, Gui Weihua, and Deconinck Geert. BIM-based PV system optimization and deployment. *Energy and Buildings*, 150(Supplement C) :13–22, September 2017.

[16] Angel A. Bayod-Rújula, Abel Ortego-Bielsa, and Amaya Martínez-Gracia. Photovoltaics on flat roofs : Energy considerations. *Energy*, 36(4) :1996–2010, April 2011.

[17] Kai Mainzer, Sven Killinger, Russell McKenna, and Wolf Fichtner. Assessment of rooftop photovoltaic potentials at the urban level using publicly available geodata and image recognition techniques. *Solar Energy*, 155(Supplement C) :561–573, October 2017.

[18] Hideki Takebayashi, Etsuko Ishii, Masakazu Moriyama, Ai Sakaki, Shunsuke Nakajima, and Hirobumi Ueda. Study to examine the potential for solar energy utilization based on the relationship between urban morphology and solar radiation gain on building rooftops and wall surfaces. *Solar Energy*, 119(Supplement C) :362–369, September 2015.

[19] Kristijan Brecl and Marko Topic. Self-shading losses of fixed free-standing pv arrays. 36 :3211–3216, 11 2011.

[20] Office Fédérale des questions conjoncturelles. Centrales Photovoltaïques - Guide pour le dimensionnement et la réalisation de projets, à l'usage des bureaux d'ingénieurs, 1996.

[21] S. Aguacil Moreno, S. Lufkin and E. Rey. Towards integrated design strategies for implementing BIPV systems into urban renewal processes : first case study in Neuchâtel (Switzerland). Sustainable Built Environment (SBE) regional conference, Zurich, Switzerland, 2016.

[22] S. Aguacil Moreno, S. Lufkin and E. Rey. Influence of energy-use scenarios in Life-Cycle Analysis of renovation projects with Building-Integrated Photovoltaics – Investigation through two case studies in Neuchâtel (Switzerland). International Conference for Sustainable Design of the Built Environment 2017, London, UK, 2017. .

[23] Service de la Géomatique et du Registre Foncier République et Canton de Neuchâtel. En route vers la 3D, 2017.

[24] G. Peronato, E. Rey, and M. Andersen. 3D-modeling of vegetation from LiDAR point clouds and assessment of its impact on façade solar irradiation. *ISPRS - International Archives of the Photogrammetry, Remote Sensing and Spatial Information Sciences*, XLII-2/W2 :67–70, 2016.

[25] Sandia National Laboratories. Photovoltaic Array Performance Model. `http://prod.sandia.gov/techlib/access-control.cgi/2004/043535.pdf`, 2004.

[26] Energie Schweiz. Calculateur solaire.

[27] Q CELLS. Q CELLS rooftop solar systems. `https://www.q-cells.co.uk/consumer/solar-systems-for-your-business/rooftopsolarsolutions.html`.

[28] Santiago Silvestre, Alfredo Boronat, and Chouder Aissa. Study of bypass diodes configuration on pv modules. pages 1632–1640, 09 2009.

[29] OFEN - Système de la rétribution unique, 2018.

[30] OFEN - Système de la rétribution de l'injection, 2018.

[31] Elcom. Votre prix de l'électricité en comparaison, 2018.

[32] Life cycle analysis of high-performance monocrystalline silicon photovoltaic systems : Energy payback times and net energy production value. `http://www.clca.columbia.edu/242_27EUPVS_Fthenakis_SunPower_6CV.4.14.pdf`, 2012.

[33] Electricity map. Emissions co2 de la consommation électrique en temps réel, 2018.

[34] Bernhard Steubing, Isabel Ballmer, Martin Gassner, Léda Gerber, Luca Pampuri, Sandro Bischof, Oliver Thees, and Rainer Zah. Identifying environmentally and economically optimal bioenergy plant sizes and locations : A spatial model of wood-based SNG value chains. *Renewable Energy*, 61 :57–68, January 2014.